

CERN-PH-EP/2015-333
2016/01/07

CMS-TOP-14-023

Measurements of $t\bar{t}$ spin correlations and top quark polarization using dilepton final states in pp collisions at $\sqrt{s} = 8$ TeV

The CMS Collaboration*

Abstract

Measurements of the top quark-antiquark ($t\bar{t}$) spin correlations and the top quark polarization are presented for $t\bar{t}$ pairs produced in pp collisions at $\sqrt{s} = 8$ TeV. The data correspond to an integrated luminosity of 19.5 fb^{-1} collected with the CMS detector at the LHC. The measurements are performed using events with two oppositely charged leptons (electrons or muons) and two or more jets, where at least one of the jets is identified as originating from a bottom quark. The spin correlations and polarization are measured from the angular distributions of the two selected leptons, both inclusively and differentially, with respect to the invariant mass, rapidity, and transverse momentum of the $t\bar{t}$ system. The measurements are unfolded to the parton level and found to be in agreement with predictions of the standard model. A search for new physics in the form of anomalous top quark chromo moments is performed. No evidence of new physics is observed, and exclusion limits on the real part of the chromo-magnetic dipole moment and the imaginary part of the chromo-electric dipole moment are evaluated.

Submitted to Physical Review D

1 Introduction

The top quark is the heaviest known elementary particle, with mass $m_t = 172.44 \pm 0.48$ GeV [1]. The top quark lifetime has been measured as $3.29_{-0.63}^{+0.90} \times 10^{-25}$ s [2], shorter than the hadronization timescale $1/\Lambda_{\text{QCD}} \approx 10^{-24}$ s, where Λ_{QCD} is the quantum chromodynamics (QCD) scale parameter, and also shorter than the spin decorrelation time scale $m_t/\Lambda_{\text{QCD}}^2 \approx 10^{-21}$ s [3]. Consequently, measurements of the angular distributions of top quark decay products give access to the spin of the top quark, allowing the precise testing of perturbative QCD in the top quark–antiquark pair ($t\bar{t}$) production process.

At the CERN LHC, top quarks are produced abundantly, predominantly in pairs. In the standard model (SM), top quarks from pair production have only a small net polarization arising from electroweak corrections to the QCD-dominated production process, but the pairs have significant spin correlations [4]. For low $t\bar{t}$ invariant masses, the production is dominated by the fusion of pairs of gluons with the same helicities, resulting in the creation of top quark pairs with antiparallel spins in the $t\bar{t}$ center-of-mass frame. For larger $t\bar{t}$ invariant masses, the dominant production is via the fusion of gluons with opposite helicities, resulting in $t\bar{t}$ pairs with parallel spins [3]. For models beyond the SM, couplings of the top quark to new particles can alter both the top quark polarization and the strength of the spin correlations in the $t\bar{t}$ system [4–7].

The charged lepton (ℓ) from the decay $t \rightarrow bW^+ \rightarrow b\ell^+\nu_\ell$ is the best spin analyzer among the top quark decay products [8], and is sensitive to the top quark spin through the helicity angle θ_ℓ^* . This is the angle of the lepton in the rest frame of its parent top quark or antiquark, measured in the helicity frame (i.e., relative to the direction of the parent quark momentum in the $t\bar{t}$ center-of-mass frame) [4].

For the decay $t\bar{t} \rightarrow b\ell^+\nu_\ell \bar{b}\ell^-\bar{\nu}_\ell$, the difference in azimuthal angle of the charged leptons in the laboratory frame, $\Delta\phi_{\ell^+\ell^-}$, is sensitive to $t\bar{t}$ spin correlations and can be measured precisely without reconstructing the full $t\bar{t}$ system [3]. With the $t\bar{t}$ system fully reconstructed, the opening angle φ between the two lepton momenta measured in the rest frames of their respective parent top quark or antiquark is directly sensitive to spin correlations, as is the product of the cosines of the helicity angles of the two leptons, $\cos\theta_{\ell^+}^* \cos\theta_{\ell^-}^*$ [4].

Recent spin correlation and polarization measurements from the CDF, D0, and ATLAS Collaborations used template fits to angular distributions, and their results were consistent with the SM expectations [9–14]. In this analysis, the measurements are made using asymmetries in angular distributions unfolded to the parton level, allowing direct comparisons between the data and theoretical predictions. The analysis strategy is similar to that presented in Ref. [15], however the larger data set used here and improvements in the $t\bar{t}$ system reconstruction techniques lead to a reduced statistical uncertainty in the measurements. Furthermore, an improved unfolding technique allows for differential measurements, which were not presented in Ref. [15].

The polarization P^\pm of the top quark (antiquark) in the helicity basis is given by $P^\pm = 2A_{P^\pm}$ [4], where the asymmetry variable A_{P^\pm} is defined as

$$A_{P^\pm} = \frac{N(\cos\theta_{\ell^\pm}^* > 0) - N(\cos\theta_{\ell^\pm}^* < 0)}{N(\cos\theta_{\ell^\pm}^* > 0) + N(\cos\theta_{\ell^\pm}^* < 0)},$$

where the numbers of events $N(\cos\theta_{\ell^\pm}^* > 0)$ and $N(\cos\theta_{\ell^\pm}^* < 0)$ are counted using the helicity angle of the positively (negatively) charged lepton in each event. Assuming CP invariance, these two measurements can be combined to give the SM polarization $P = 2A_P = (A_{P^+} + A_{P^-})$. Alternatively, the variable $P^{\text{CPV}} = 2A_P^{\text{CPV}} = (A_{P^+} - A_{P^-})$ measures possible

polarization introduced by a maximally CP-violating process [4].

For $t\bar{t}$ spin correlations, the variable

$$A_{\Delta\phi} = \frac{N(|\Delta\phi_{\ell^+\ell^-}| > \pi/2) - N(|\Delta\phi_{\ell^+\ell^-}| < \pi/2)}{N(|\Delta\phi_{\ell^+\ell^-}| > \pi/2) + N(|\Delta\phi_{\ell^+\ell^-}| < \pi/2)}$$

discriminates between correlated and uncorrelated t and \bar{t} spins, while the variable

$$A_{c_1c_2} = \frac{N(c_1c_2 > 0) - N(c_1c_2 < 0)}{N(c_1c_2 > 0) + N(c_1c_2 < 0)},$$

where $c_1 = \cos\theta_{\ell^+}^*$ and $c_2 = \cos\theta_{\ell^-}^*$, provides a direct measure of the spin correlation coefficient C_{hel} through the relationship $C_{\text{hel}} = -4A_{c_1c_2}$ [4]. The variable

$$A_{\cos\varphi} = \frac{N(\cos\varphi > 0) - N(\cos\varphi < 0)}{N(\cos\varphi > 0) + N(\cos\varphi < 0)}$$

provides a direct measure of the spin correlation coefficient D by the relation $D = -2A_{\cos\varphi}$ [4].

In addition to the inclusive measurements, we determine the asymmetries differentially as a function of three variables describing the $t\bar{t}$ system in the laboratory frame: its invariant mass $M_{t\bar{t}}$, rapidity $y_{t\bar{t}}$, and transverse momentum $p_T^{t\bar{t}}$. The results presented in this paper are based on data collected by the CMS experiment at the LHC, corresponding to an integrated luminosity of 19.5 fb^{-1} from pp collisions at $\sqrt{s} = 8 \text{ TeV}$.

2 The CMS detector

The central feature of the CMS apparatus is a superconducting solenoid of 6 m internal diameter, providing a magnetic field of 3.8 T. Within the solenoid volume are a silicon pixel and strip tracker, a lead tungstate crystal electromagnetic calorimeter, and a brass and scintillator hadron calorimeter, each composed of a barrel and two endcap sections. Forward calorimeters extend the pseudorapidity coverage provided by the barrel and endcap detectors. Muons are measured in gas-ionization detectors embedded in the steel flux-return yoke outside the solenoid. The first level of the CMS trigger system, composed of custom hardware processors, uses information from the calorimeters and muon detectors to select the most interesting events in a fixed time interval of less than $4 \mu\text{s}$. The high-level trigger processor farm further decreases the event rate from around 100 kHz to less than 1 kHz, before data storage. A more detailed description of the CMS detector, together with a definition of the coordinate system used and the relevant kinematic variables, can be found in Ref. [16].

3 Event samples

3.1 Object definition and event selection

Events are selected using triggers that require the presence of at least two leptons (electrons or muons) with transverse momentum (p_T) greater than 17 GeV for the highest- p_T lepton and 8 GeV for the second-highest p_T lepton. The trigger efficiency per lepton, measured relative to the full offline lepton selection detailed in this section using a data sample of Drell-Yan ($Z/\gamma^* \rightarrow \ell\ell$) events, is about 98% (96%) for electrons (muons), with variations at the level of several percent depending on the pseudorapidity η and p_T of the lepton.

The particle-flow (PF) algorithm [17, 18] is used to reconstruct and identify each individual particle with an optimized combination of information from the various elements of the CMS detector. The offline selection requires events to have exactly two leptons of opposite charge with $p_T > 20$ GeV and $|\eta| < 2.4$. Electron candidates are reconstructed starting from a cluster of energy deposits in the electromagnetic calorimeter. The cluster is then matched to a reconstructed track. The electron selection is based on the shower shape, track-cluster matching, and consistency between the cluster energy and the track momentum [19]. Muon candidates are reconstructed by performing a global fit that requires consistent hit patterns in the silicon tracker and the muon system [20].

The events with an e^+e^- or $\mu^+\mu^-$ pair having an invariant mass, $M_{\ell\ell}$, within 15 GeV of the Z boson mass are removed to suppress the Drell–Yan background. For all events, we require $M_{\ell\ell} > 20$ GeV. Leptons are required to be isolated from other activity in the event. The lepton isolation is measured using the scalar p_T sum (p_T^{sum}) of all PF particles not associated with the lepton within a cone of radius $\Delta R \equiv \sqrt{(\Delta\eta)^2 + (\Delta\phi)^2} = 0.3$, where $\Delta\eta$ ($\Delta\phi$) is the distance in η (ϕ) between the directions of the lepton and the PF particle at the primary interaction vertex [21]. The average contribution of particles from additional pp interactions in the same or nearby bunch crossings (pileup) is estimated and subtracted from the p_T^{sum} quantity. The isolation requirement is $p_T^{\text{sum}} < \min(5 \text{ GeV}, 0.15 p_T^\ell)$, where p_T^ℓ is the lepton p_T . Typical lepton identification and isolation efficiencies, measured in samples of Drell–Yan events [22], are 76% for electrons and 91% for muons, with variations at the level of several percent within the p_T and η ranges of the selected leptons.

The PF particles are clustered to form jets using the anti- k_T clustering algorithm [23] with a distance parameter of 0.5, as implemented in the FASTJET package [24]. The contribution to the jet energy from pileup is estimated on an event-by-event basis using the jet-area method described in Ref. [25], and is subtracted from the overall jet p_T . Jets from pileup interactions are suppressed using a multivariate discriminant based on the multiplicity of objects clustered in the jet, the jet shape, and the impact parameters of the charged tracks in the jet with respect to the primary interaction vertex. The jets must be separated from the selected leptons by $\Delta R > 0.4$.

The selected events are required to contain at least two jets with $p_T > 30$ GeV and $|\eta| < 2.4$. At least one of these jets must be consistent with containing the decay of a bottom (b) flavored hadron, as identified using the medium operating point of the combined secondary vertex (CSV) b quark tagging algorithm [26]. We refer to such jets as b-tagged jets. The efficiency of this algorithm for b quark jets in the p_T range 30–400 GeV is 60–75% for $|\eta| < 2.4$. The misidentification rate for light-quark or gluon jets is approximately 1% for the chosen working point [26].

The missing transverse momentum vector \vec{p}_T^{miss} is defined as the projection on the plane perpendicular to the beam direction of the negative vector sum of the momenta of all reconstructed particles in the event. Its magnitude is referred to as E_T^{miss} . The calibrations that are applied to the energy measurements of jets are propagated to a correction of \vec{p}_T^{miss} . The E_T^{miss} value is required to exceed 40 GeV in events with same-flavor leptons in order to further suppress the Drell–Yan background. There is no E_T^{miss} requirement for $e^\pm\mu^\mp$ events.

3.2 Signal and background simulation

Simulated signal $t\bar{t}$ events with a top quark mass of $m_t = 172.5$ GeV and with SM spin correlations are generated using the MC@NLO 3.41 [27, 28] Monte Carlo (MC) event generator with the CTEQ6M parton distribution functions (PDF) [29]. The parton showering and frag-

mentation are performed by HERWIG 6.520 [30]. Simulations with different values of m_t and renormalization and factorization scales (μ_R and μ_F) are used to evaluate the associated systematic uncertainties. Background samples of $W + \text{jets}$, Drell–Yan, diboson (WW , WZ , and ZZ), triboson, and $t\bar{t} + \text{boson}$ events are generated with MADGRAPH 5.1.3.30 [31, 32], and normalized to the calculated next-to-leading-order (NLO) [33–37] or next-to-next-to-leading-order (NNLO) [38] cross sections. Single top quark events are generated using POWHEG 1.0 [39–41], and normalized to the theoretical NNLO cross sections [42–46]. For the background samples and an alternative $t\bar{t}$ sample generated using POWHEG 1.0, the parton showering and fragmentation are done using PYTHIA 6.4.22 [47].

For both signal and background events, pileup interactions are simulated with PYTHIA and superimposed on the hard collisions using a pileup multiplicity distribution that reflects the luminosity profile of the analyzed data. The CMS detector response is simulated using a GEANT4-based model [48]. The simulated events are reconstructed and analyzed with the same software used to process the collision data.

The measured trigger efficiencies are used to weight the simulated events to account for the trigger requirement. Small differences between the b tagging efficiencies measured in data and simulation [26] are accounted for by using data-to-simulation correction factors to adjust the b tagging probability in simulated events, while the lepton selection efficiencies (reconstruction, identification, and isolation) are found to be consistent between data and simulation [22].

4 Background estimation

Control regions (CR) are used to validate the background estimates from simulation and derive scale factors (SF) and systematic uncertainties for some background processes. Each SF multiplies the simulated background yield for the given process in the signal region (SR) to obtain the final background prediction. The CRs are designed to have similar kinematics to the SR, but with one or two selection requirements reversed, thus enhancing different SM contributions. The main CRs used in this analysis and the values of the derived SFs are summarized in Table 1.

Table 1: Descriptions of the various control regions, their intended background process, and the scale factors derived from them, including either the statistical and systematic uncertainties or the total uncertainty. The last row gives the scale factor used for all the remaining backgrounds, whose contributions are estimated from simulation alone.

Selection change with respect to the signal region	Target background process	Scale factor
ee or $\mu\mu$ only, $76 < M_{\ell\ell} < 106 \text{ GeV}$	$Z/\gamma^*(\rightarrow ee/\mu\mu) + \text{jets}$	$1.36 \pm 0.02 \text{ (stat)} \pm 0.2 \text{ (syst)}$
ee or $\mu\mu$ only, no E_T^{miss} req., $76 < M_{\ell\ell} < 106 \text{ GeV}$	$Z/\gamma^*(\rightarrow \tau\tau) + \text{jets}$	$1.18 \pm 0.01 \text{ (stat)} \pm 0.1 \text{ (syst)}$
Same-charge leptons	One-lepton processes	$2.2 \pm 0.3 \text{ (stat)} \pm 1.0 \text{ (syst)}$
Exactly one jet	Single top quark (tW , 2 leptons)	$1.00 \pm 0.25 \text{ (total)}$
Simulation	All other backgrounds	$1.0 \pm 0.5 \text{ (total)}$

Table 2: Predicted background and observed event yields, with their statistical uncertainties, after applying the event selection criteria and normalization described in the text.

Sample	ee	$\mu\mu$	$e\mu$	Total
Single top quark (tW, 2 leptons)	298.0 ± 1.6	425.9 ± 1.9	1161.9 ± 3.1	1885.8 ± 4.0
Single top quark (other)	2.6 ± 0.6	4.6 ± 0.9	18.8 ± 1.6	26.1 ± 1.9
$t\bar{t} \rightarrow \ell + \text{jets}$	107.1 ± 7.7	62.2 ± 5.4	327 ± 13	497 ± 16
W + jets	7.3 ± 3.6	1.8 ± 1.8	10.0 ± 3.5	19.1 ± 5.3
$Z/\gamma^*(\rightarrow ee/\mu\mu) + \text{jets}$	211 ± 16	368 ± 23	1.6 ± 0.5	581 ± 28
$Z/\gamma^*(\rightarrow \tau\tau) + \text{jets}$	33.9 ± 2.5	51.5 ± 3.0	137.6 ± 5.1	223.0 ± 6.4
WW/WZ/ZZ	27.6 ± 1.4	40.7 ± 1.4	89.3 ± 2.3	157.5 ± 3.0
Triboson	1.5 ± 0.1	2.3 ± 0.2	5.2 ± 0.3	9.0 ± 0.4
$t\bar{t}W/t\bar{t}Z/t\bar{t}\gamma$	86.4 ± 6.5	141.3 ± 8.2	332 ± 13	559 ± 17
Total background	775 ± 20	1098 ± 25	2083 ± 20	3957 ± 38
Data	7089	10074	26735	43898
Signal yield (data – background)	6314 ± 86	8980 ± 100	24650 ± 160	39940 ± 210

For Drell–Yan events, the SF accounts for mismodeling of the E_T^{miss} distribution (coming largely from mismeasured jets) and mismodeling of the heavy-flavor content. Only the latter is relevant for $Z/\gamma^*(\rightarrow \tau\tau) + \text{jets}$, where the E_T^{miss} is dominated by the well-modeled undetected neutrinos, so we omit the E_T^{miss} mismodeling in the derivation of the SF for this process. The systematic uncertainties in the SFs are taken from the envelope of the variation observed between the three dilepton flavor combinations and in various alternative CRs. The CR for single top quark production in association with a W boson (tW) is still dominated by signal events (75%), with only a 16% contribution from tW production, which is an enhancement by a factor of 4 compared to the SR. Given the good agreement between data and simulation in this CR, we assume a SF of unity for tW production, with an uncertainty of 25% based on the recent CMS tW cross section measurement of 23.4 ± 5.4 pb [49].

Contributions to the background from diboson and triboson production, as well as $t\bar{t}$ production in association with a boson, are estimated from simulation. Recent measurements from the CMS Collaboration [50–52] indicate agreement between the predicted and measured cross sections for these processes, and we assign a systematic uncertainty of 50%.

5 Event yields and measurements at the reconstruction level

The expected background and observed event yields for different dilepton flavor combinations are listed in Table 2. The total predicted yield in the $e\mu$ channel is significantly larger than for the same-flavor channels because of the additional requirements on E_T^{miss} and $M_{\ell\ell}$ described in Section 3 that are applied to suppress the Drell–Yan background. After subtraction of the predicted background yields, the remaining yield in the data is assumed to be signal from dileptonic $t\bar{t}$ decays, including τ leptons that decay leptonically. All other $t\bar{t}$ decay modes are treated as background and are included in the $t\bar{t} \rightarrow \ell + \text{jets}$ category. The largest background comes from tW production with dileptonic decays.

While the $|\Delta\phi_{\ell^+\ell^-}|$ measurement relies only on the leptonic information, the measurements based on $\cos\varphi$ and $\cos\theta_{\ell^\pm}^*$ require the reconstruction of the entire $t\bar{t}$ system. Each signal event has two neutrinos in the final state, and there is also a twofold ambiguity in combining the b quark jets with the leptons. In the case of events with only one b-tagged jet (62% of the

selected events), the untagged jet with the highest b quark likelihood from the CSV algorithm is assumed to be the second b quark jet. The two neutrino momenta are found analytically assuming $m_t = 172.5 \text{ GeV}$. In the case of events with no physical solutions, a geometrical method is used to find the physical solution with the magnitude of the vector sum of the p_T of the two neutrinos as close as possible to the measured E_T^{miss} [53]. Each event has up to 8 possible solutions. The one most likely to represent the correct $t\bar{t}$ configuration is chosen based on the probabilities to observe the lepton energies in their parent top quark rest frames and the extracted Bjorken x values of the initial-state partons [54]. No solutions are found for 16% of the events, both in the data and the simulation. These events are not used, except in the inclusive measurement of $|\Delta\phi_{\ell^+\ell^-}|$.

A comparison of the distributions for the reconstructed $t\bar{t}$ system variables $M_{t\bar{t}}$, $y_{t\bar{t}}$, and $p_T^{t\bar{t}}$ between data and simulation is shown in Fig. 1, where the signal yield from the simulation has been normalized to the number of signal events in the data after background subtraction. In general, the shapes of the distributions from data and simulation show reasonable agreement, with the small discrepancies covered by the systematic variations in the top quark p_T modeling, PDFs, and μ_R and μ_F values, which will be discussed in Section 7. A similar comparison of the angular distributions is shown in Fig. 2. The corresponding inclusive asymmetry values, uncorrected for background, from the data and simulation are given in Table 3.

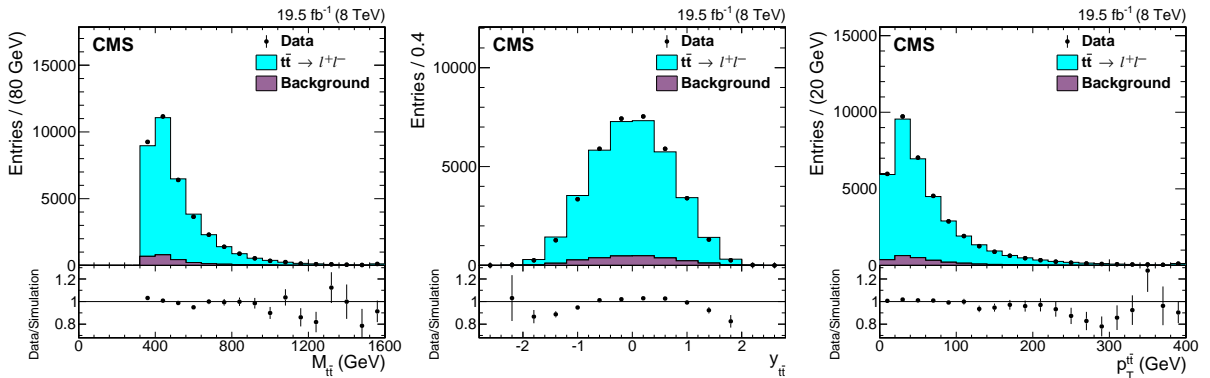


Figure 1: Reconstructed $M_{t\bar{t}}$, $y_{t\bar{t}}$, and $p_T^{t\bar{t}}$ distributions from data (points) and simulation (histogram), with the expected signal ($t\bar{t} \rightarrow \ell^+\ell^-$) and background distributions shown separately. All three dilepton flavor combinations are included. The simulated signal yield is normalized to that of the background-subtracted data. The last bins of the $M_{t\bar{t}}$ and $p_T^{t\bar{t}}$ distributions include overflow events. The vertical bars on the data points represent the statistical uncertainties. The lower panels show the ratio of the numbers of events from data and simulation.

Table 3: Values of the uncorrected inclusive asymmetry variables from simulation and data, prior to background subtraction. The uncertainties shown are statistical.

Reconstructed asymmetry	Simulation	Data
$A_{\Delta\phi}$	0.188 ± 0.002	0.170 ± 0.005
$A_{\cos\varphi}$	0.114 ± 0.003	0.109 ± 0.005
$A_{c_1c_2}$	-0.050 ± 0.003	-0.049 ± 0.005
A_{P+}	-0.026 ± 0.003	-0.032 ± 0.005
A_{P-}	-0.022 ± 0.003	-0.028 ± 0.005

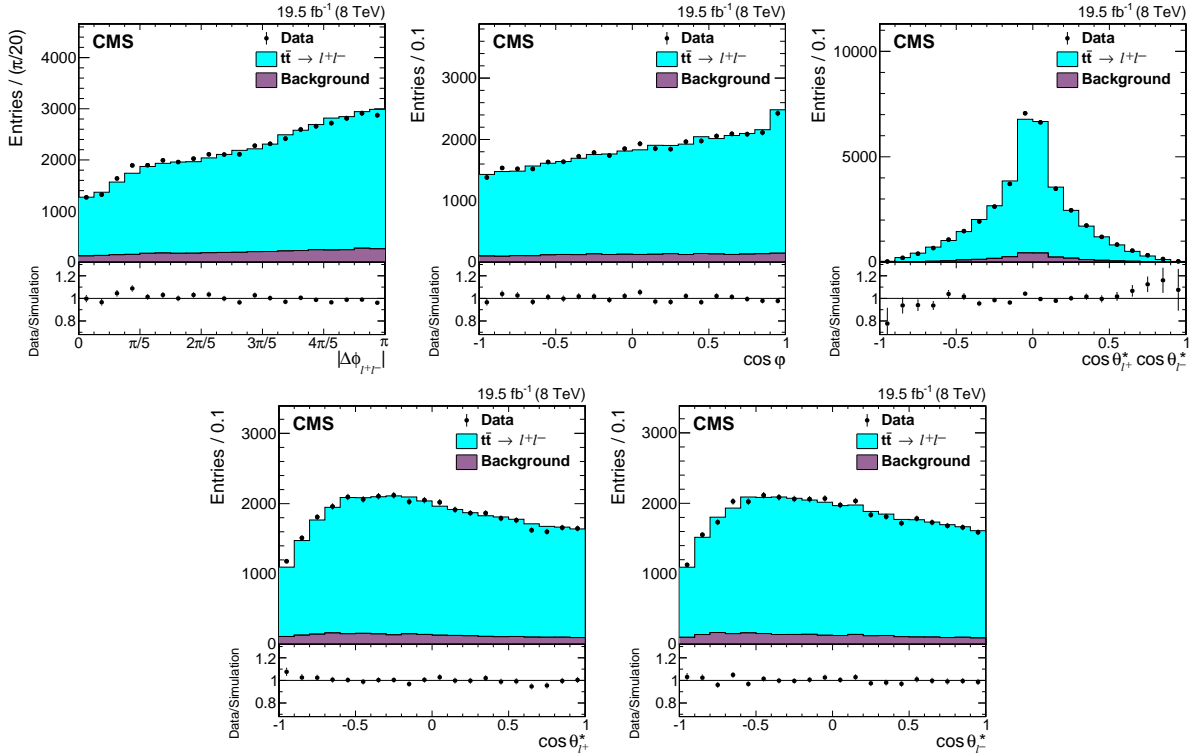


Figure 2: Reconstructed angular distributions from data (points) and simulation (histogram), with the expected signal ($t\bar{t} \rightarrow \ell^+\ell^-$) and background distributions shown separately. All three dilepton flavor combinations are included. The simulated signal yield is normalized to that of the background-subtracted data. The vertical bars on the data points represent the statistical uncertainties. The lower panels show the ratio of the numbers of events from data and simulation.

6 Unfolding the distributions

The observed angular distributions are distorted compared to the underlying distributions at the parton level (for which theoretical predictions exist) by the detector acceptance and resolution and the trigger and event selection efficiencies. To correct the data for these effects, we apply an unfolding procedure that yields the corrected $|\Delta\phi_{\ell^+\ell^-}|$, $\cos\varphi$, c_1c_2 , and $\cos\theta_{\ell^\pm}^*$ distributions at the parton level. In the context of theoretical calculations and parton-shower event generators, the parton-level top quark is defined before it decays, and its kinematics include the effects of recoil from initial- and final-state radiation in the rest of the event and from final-state radiation from the top quark itself. The parton-level charged lepton, produced from the decay of the intermediate W boson, is defined before the lepton radiates any photons or the muon or tau lepton decays.

In order to unfold the observed distributions it is necessary to choose a binning scheme. Aiming to have bins with widths well matched to the reconstruction resolution and with approximately uniform event contents, we select six bins for each parton-level angular distribution except that of $\Delta\phi_{\ell^+\ell^-}$. This variable depends only on the lepton momentum measurements, not on the reconstruction of the $t\bar{t}$ system, and the superior resolution allows us to use twelve bins. For the reconstruction-level distributions we use twice as many bins as for the parton-level distributions.

The background-subtracted distribution for each variable, considered as a vector \vec{y} , is related to the underlying parton-level distribution \vec{x} through the equation $\vec{y} = SA\vec{x}$, where A is a diagonal matrix describing the fraction (acceptance times efficiency) of all produced signal events that are expected to be selected in each of the measured bins, and S is a non-diagonal “smearing” matrix describing the migration of events between bins caused by imperfect detector resolution and reconstruction techniques. The A and S matrices are constructed using simulated MC@NLO $t\bar{t}$ events. The smearing in $\cos\varphi$, c_1c_2 , and $\cos\theta_{\ell^\pm}^*$ can be large in some events because of the uncertainties in the reconstruction of the $t\bar{t}$ kinematic quantities, but the smearing matrices are still predominantly diagonal. The smearing matrix for $|\Delta\phi_{\ell^+\ell^-}|$ is nearly diagonal because of the excellent angular resolution of the lepton momentum measurements.

To determine the parton-level angular distribution in data, we employ a regularized unfolding algorithm implemented in the TUNFOLD package [55]. The effects of large statistical fluctuations in the algorithm are greatly reduced by introducing a term in the unfolding procedure that regularizes the output distribution based on the curvature of the simulated signal distribution. In general, unfolding introduces negative correlations between adjacent bins, while regularization introduces positive correlations, and the regularization strength is optimized by minimizing the average global correlation coefficient in the unfolded distribution. The regularization strength obtained here is relatively weak, contributing at the 10% level to the total χ^2 minimized by the algorithm.

After unfolding, each distribution is normalized to unit area to give the normalized differential cross section for each variable. We use an analogous unfolding procedure to measure the normalized double-differential cross section, using three bins of $M_{t\bar{t}}$, $|y_{t\bar{t}}|$, and $p_T^{t\bar{t}}$ for each variable. The full covariance matrix is used in the evaluation of the statistical uncertainty in the asymmetry measured from each distribution.

7 Systematic uncertainties

The systematic uncertainties coming from the detector performance and the modeling of the signal and background processes are evaluated from the difference between the nominal measurement and that obtained by repeating the unfolding procedure using simulated events with the appropriate systematic variation.

The uncertainty from the jet energy scale (JES) corrections affects the $t\bar{t}$ final-state reconstruction, as well as the event selection. It is estimated by varying the energies of jets within their uncertainties [56], and propagating this to the E_T^{miss} value. Similarly, the jet energy resolution is varied by 2–5%, depending on the η of the jet [56], and the electron energy scale is varied by $\pm 0.6\%$ ($\pm 1.5\%$) for barrel (endcap) electrons (the uncertainty in muon energies is negligible), as estimated from comparisons between measured and simulated Drell–Yan events [57].

The uncertainty in the background contribution is obtained by varying the normalization of each background component by the uncertainties described in Section 4.

Many of the signal modeling and simulation uncertainties are evaluated by using weights to vary the MC@NLO $t\bar{t}$ sample: the simulated pileup multiplicity distribution is changed within its uncertainty; the correction factors between data and simulation for the b tagging [26], trigger, and lepton selection efficiencies are shifted up and down by their uncertainties; and the PDFs are varied using the PDF4LHC procedure [58, 59]. Previous CMS studies [60, 61] have shown that the p_T distribution of the top quark measured from data is softer than that in the NLO simulation of $t\bar{t}$ production. Since the origin of the discrepancy is not fully understood, the change in the measurement when reweighting the MC@NLO $t\bar{t}$ sample to match the top quark p_T spectrum in data is taken as a systematic uncertainty associated with signal modeling.

The remaining signal modeling uncertainties are separately evaluated with dedicated $t\bar{t}$ samples: μ_R and μ_F are varied together up and down by a factor of 2; the top quark mass is varied by ± 1 GeV, to be consistent with the uncertainty used in other CMS measurements with the $\sqrt{s} = 8$ TeV data set (the effect on the total systematic uncertainty of using the reduced uncertainty from the recent CMS combined m_t measurement [1] would be negligible); and the S matrix is rederived from a $t\bar{t}$ sample generated with POWHEG and PYTHIA, while the A matrix is unchanged, in order to estimate the difference in hadronization modeling between HERWIG and PYTHIA. To avoid underestimation of systematic uncertainties caused by statistical fluctuations, which can be significant in the estimates evaluated using dedicated $t\bar{t}$ samples, for each source of uncertainty the maximum of the estimated systematic uncertainty and the statistical uncertainty in that estimate is taken as the final systematic uncertainty.

The uncertainty in the unfolding procedure is dominated by the statistical uncertainty arising from the finite number of events in the MC@NLO $t\bar{t}$ sample. The uncertainty owing to the unfolding regularization is evaluated by using the reconstructed distribution of a variable in data to reweight the corresponding simulated signal distribution used to regularize the curvature of the unfolded distribution. Using this method, the regularization uncertainty is found to be negligible for all measurements.

The systematic uncertainties in the inclusive asymmetry variables obtained from the unfolded distributions are summarized in Table 4. The systematic uncertainties are evaluated for each bin of the unfolded distributions, from which the covariance matrix is constructed, assuming 100% correlation or anticorrelation between bins for each individual source of uncertainty. The total systematic uncertainty is calculated by adding in quadrature the listed uncertainties.

Table 4: Sources and values of the systematic uncertainties in the inclusive asymmetry variables.

Asymmetry variable	$A_{\Delta\phi}$	$A_{\cos\varphi}$	$A_{c_1c_2}$	A_P	A_P^{CPV}
Experimental systematic uncertainties					
Jet energy scale	0.001	0.005	0.007	0.018	0.001
Jet energy resolution	<0.001	0.001	0.002	0.003	0.002
Lepton energy scale	0.001	0.002	0.005	0.003	<0.001
Background	0.001	0.001	0.001	0.002	<0.001
Pileup	<0.001	<0.001	<0.001	<0.001	<0.001
b tagging efficiency	<0.001	0.001	0.001	0.001	0.001
Lepton selection	0.001	<0.001	<0.001	0.002	<0.001
$t\bar{t}$ modeling uncertainties					
Parton distribution functions	0.004	0.005	0.005	0.001	<0.001
Top quark p_T	0.011	0.006	0.006	0.004	<0.001
Fact. and renorm. scales	0.002	0.003	0.005	0.002	0.002
Top quark mass	0.001	0.001	0.007	0.008	0.001
Hadronization	0.001	0.004	0.005	0.019	0.003
Unfolding (simulation statistical)	0.002	0.005	0.006	0.003	0.003
Unfolding (regularization)	<0.001	<0.001	<0.001	<0.001	<0.001
Total systematic uncertainty	0.012	0.012	0.016	0.028	0.005

For $A_{\Delta\phi}$, the top quark p_T modeling uncertainty dominates; this arises from the dependence of the $|\Delta\phi_{\ell^+\ell^-}|$ distribution shape on the top quark p_T (through the spin correlations and event kinematics); that, in turn, introduces a significant dependence of the acceptance correction on the top quark p_T . For A_P , the JES and hadronization systematic uncertainties are dominant. Both affect the reconstructed b quark jet energy, and can therefore bias the boost from the laboratory frame to the top quark center-of-mass frame, and thus the measurement of $\cos\theta_{\ell^\pm}^*$. For similar reasons, the same two uncertainties are large for $A_{c_1c_2}$ and $A_{\cos\varphi}$, which are also significantly affected by the top quark p_T modeling uncertainty through its effect on the spin correlations. For A_P^{CPV} , the similar systematic uncertainties in A_{P+} and A_{P-} largely cancel when A_{P-} is subtracted from A_{P+} ; the remaining contributions to the systematic uncertainty are dominated by the statistical uncertainty in the simulation.

8 Results

8.1 Unfolded distributions

The background-subtracted, unfolded, and normalized-to-unit-area angular distributions for the selected data events are shown in Fig. 3, along with the parton-level predictions obtained with the MC@NLO event generator and from NLO QCD calculations including electroweak corrections (NLO+EW) for $t\bar{t}$ production, with and without spin correlations [4, 62].

The measured asymmetries, obtained from the angular distributions unfolded to the parton level, are presented with their statistical and systematic uncertainties in Table 5, where they are compared to predictions from MC@NLO and the NLO+EW calculations. Correlations between the contents of different bins, introduced by the unfolding process and from the systematic uncertainties, are accounted for in the calculation of the experimental uncertainties. The uncertainties in the NLO+EW predictions come from varying μ_R and μ_F simultaneously up and

down by a factor of two. For $A_{\cos\varphi}$ and $A_{c_1c_2}$, these scale uncertainties are summed in quadrature with the difference between the NLO+EW predictions from Ref. [4] when the ratio in the calculation is expanded in powers of the strong coupling constant and when the numerator and denominator are evaluated separately.

Table 5: Inclusive asymmetry measurements obtained from the angular distributions unfolded to the parton level, and the parton-level predictions from the MC@NLO simulation and from NLO+EW calculations with (SM) and without (no spin corr.) spin correlations [4, 62]. For the data, the first uncertainty is statistical and the second is systematic. For the MC@NLO results and NLO+EW calculations, the uncertainties are statistical and theoretical, respectively.

Asymmetry variable	Data (unfolded)	MC@NLO simulation	NLO+EW, SM	NLO+EW, no spin corr.
$A_{\Delta\phi}$	$0.094 \pm 0.005 \pm 0.012$	0.113 ± 0.001	$0.110^{+0.006}_{-0.009}$	$0.202^{+0.006}_{-0.009}$
$A_{\cos\varphi}$	$0.102 \pm 0.010 \pm 0.012$	0.114 ± 0.001	0.114 ± 0.006	0
$A_{c_1c_2}$	$-0.069 \pm 0.013 \pm 0.016$	-0.081 ± 0.001	-0.080 ± 0.004	0
A_P	$-0.011 \pm 0.007 \pm 0.028$	0	0.002 ± 0.001	—
A_P^{CPV}	$0.000 \pm 0.006 \pm 0.005$	0	0	—

Using the relationships between the asymmetry variables and spin correlation coefficients given in Section 1, we find $C_{\text{hel}} = 0.278 \pm 0.084$ and $D = 0.205 \pm 0.031$, where the uncertainties include the statistical and systematic components added in quadrature. Similarly, the CP-conserving and CP-violating components of the top quark polarization are found to be $P = -0.022 \pm 0.058$ and $P^{\text{CPV}} = 0.000 \pm 0.016$, respectively. All measurements are consistent with the expectations of the SM.

The NLO+EW predictions for $|\Delta\phi_{\ell^+\ell^-}|$, $\cos\varphi$, and c_1c_2 with and without spin correlations in Table 5 are used to translate the measurements into determinations of f_{SM} , the strength of the spin correlations relative to the SM prediction, with $f_{\text{SM}} = 1$ corresponding to the SM and $f_{\text{SM}} = 0$ corresponding to uncorrelated events. The measurements of f_{SM} are shown in Table 6 and are derived under the assumption that the acceptance matrix for unfolding is independent of spin correlations. This is found to give conservative estimates for the experimental uncertainties.

Table 6: Values of f_{SM} , the strength of the measured spin correlations relative to the SM prediction, derived from the numbers in Table 5. The last row shows an additional measurement of f_{SM} made from the projection in $|\Delta\phi_{\ell^+\ell^-}|$ of the normalized double-differential cross section as a function of $|\Delta\phi_{\ell^+\ell^-}|$ and $M_{\text{t}\bar{\text{t}}}$. The uncertainties shown are statistical, systematic, and theoretical, respectively. The total uncertainty in each result, found by adding the individual uncertainties in quadrature, is shown in the last column.

Variable	$f_{\text{SM}} \pm (\text{stat}) \pm (\text{syst}) \pm (\text{theor})$	Total uncertainty
$A_{\Delta\phi}$	$1.14 \pm 0.06 \pm 0.13^{+0.08}_{-0.11}$	$^{+0.16}_{-0.18}$
$A_{\cos\varphi}$	$0.90 \pm 0.09 \pm 0.10 \pm 0.05$	± 0.15
$A_{c_1c_2}$	$0.87 \pm 0.17 \pm 0.21 \pm 0.04$	± 0.27
$A_{\Delta\phi} \text{ (vs. } M_{\text{t}\bar{\text{t}}}\text{)}$	$1.12 \pm 0.06 \pm 0.08^{+0.08}_{-0.11}$	$^{+0.12}_{-0.15}$

The dependence of each asymmetry on $M_{\text{t}\bar{\text{t}}}$, $|y_{\text{t}\bar{\text{t}}}|$, and $p_{\text{T}}^{\text{t}\bar{\text{t}}}$ is extracted from the measured normalized double-differential cross section, and the results are shown in Fig. 4. The measurements are all consistent with the MC@NLO predictions, and with the SM NLO+EW prediction for the $M_{\text{t}\bar{\text{t}}}$ and $|y_{\text{t}\bar{\text{t}}}|$ dependencies. No comparison is made with the NLO+EW prediction for the $p_{\text{T}}^{\text{t}\bar{\text{t}}}$ dependence because the substantial effect of the parton shower on the $p_{\text{T}}^{\text{t}\bar{\text{t}}}$ distribution means fixed-order NLO calculations are not a sufficiently good approximation of the data.

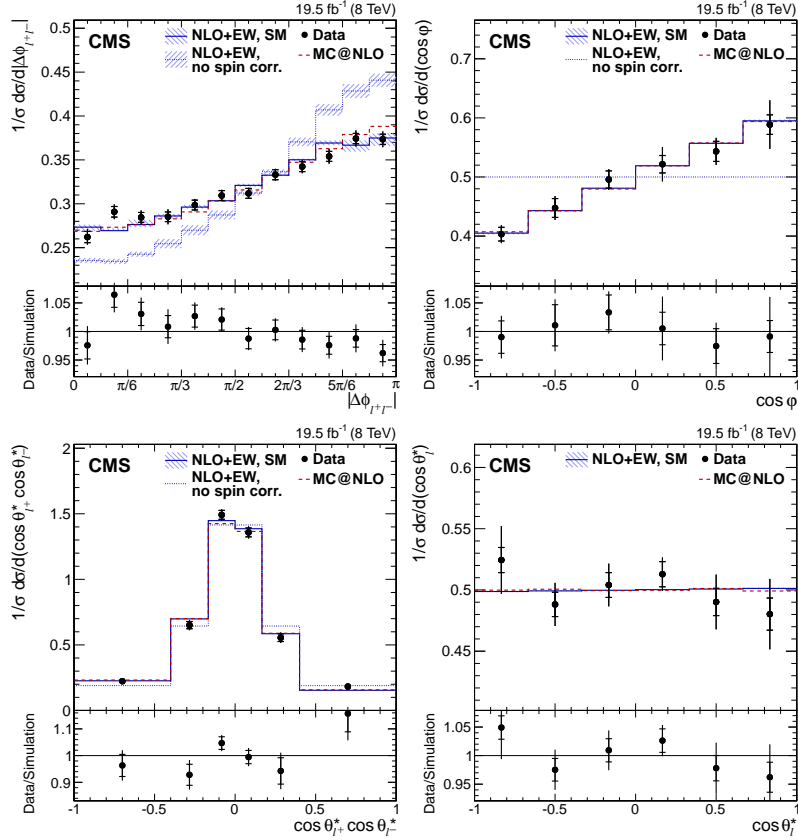


Figure 3: Normalized differential cross section as a function of $|\Delta\phi_{\ell^+\ell^-}|$, $\cos\phi$, $\cos\theta_{\ell^+}^*\cos\theta_{\ell^-}^*$, and $\cos\theta_\ell^*$ from data (points); parton-level predictions from MC@NLO (dashed histograms); and theoretical predictions at NLO+EW [4, 62] with (SM) and without (no spin corr.) spin correlations (solid and dotted histograms, respectively). For the $\cos\theta_\ell^*$ distribution, CP conservation is assumed in the combination of the $\cos\theta_{\ell^\pm}^*$ measurements from positively and negatively charged leptons. The ratio of the data to the MC@NLO prediction is shown in the lower panels. The inner and outer vertical bars on the data points represent the statistical and total uncertainties, respectively. The hatched bands represent variations of μ_R and μ_F simultaneously up and down by a factor of two.

Compared to the measurement of $A_{\Delta\phi}$ in Table 5, the differential measurement in bins of $M_{t\bar{t}}$ (Fig. 4, top row, left plot) has a significantly reduced (factor of 2.3) systematic uncertainty associated with the top quark p_T modeling. When the acceptance correction is binned in a variable that is correlated with the top quark p_T (e.g., $M_{t\bar{t}}$), the top quark p_T reweighting affects the numerator and denominator in the acceptance ratio similarly, leading to a reduction in the associated systematic uncertainty. The inclusive asymmetry measured from the projection in $|\Delta\phi_{\ell+\ell-}|$ of the normalized double-differential cross section is $A_{\Delta\phi} = 0.095 \pm 0.006$ (stat) ± 0.007 (syst), which is converted into the value of $f_{\text{SM}} = 1.12^{+0.12}_{-0.15}$ given in Table 6.

8.2 Limits on new physics

Anomalous $t\bar{t}g$ couplings can lead to a significant modification of the polarization and spin correlations in $t\bar{t}$ events. A model-independent search can be performed using an effective model of chromo-magnetic and chromo-electric dipole moments (denoted CMDM and CEDM, respectively). This study follows the proposal in Ref. [4]. For an anomalous $t\bar{t}g$ interaction arising from heavy-particle exchange characterized by a mass scale $M \gtrsim m_t$, one can write an effective Lagrangian as:

$$\mathcal{L}_{\text{eff}} = -\frac{\tilde{\mu}_t}{2} \bar{t} \sigma^{\mu\nu} T^a t G_{\mu\nu}^a - \frac{\tilde{d}_t}{2} \bar{t} i \sigma^{\mu\nu} \gamma_5 T^a t G_{\mu\nu}^a, \quad (1)$$

where $\tilde{\mu}_t$ and \tilde{d}_t are the CMDM (CP-conserving) and CEDM (CP-violating) dipole moments, $G_{\mu\nu}^a$ is the gluon field strength, and T^a are the QCD fundamental generators. It is usually preferred to define dimensionless parameters

$$\hat{\mu}_t \equiv \frac{m_t}{g_s} \tilde{\mu}_t, \quad \hat{d}_t \equiv \frac{m_t}{g_s} \tilde{d}_t, \quad (2)$$

where g_s is the QCD coupling constant [4]. The parameters $\hat{\mu}_t$ and \hat{d}_t correspond to the form factors in the time-like kinematic domain and are therefore complex quantities, here assumed to be constant. In general, both the real and imaginary parts of $\hat{\mu}_t$ and \hat{d}_t can be determined, but the spin correlations and polarization measured in this paper are only sensitive to $\text{Re}(\hat{\mu}_t)$ and $\text{Im}(\hat{d}_t)$, respectively [4].

We begin with the determination of $\text{Re}(\hat{\mu}_t)$ using the measured normalized differential cross section $(1/\sigma)(d\sigma/d|\Delta\phi_{\ell+\ell-}|)$. In the presence of a small new physics (NP) contribution such that $\text{Re}(\hat{\mu}_t) \ll 1$, one can linearly expand the normalized differential cross section as [4]:

$$\frac{1}{\sigma} \frac{d\sigma}{d|\Delta\phi_{\ell+\ell-}|} = \left(\frac{1}{\sigma} \frac{d\sigma}{d|\Delta\phi_{\ell+\ell-}|} \right)_{\text{SM}} + \text{Re}(\hat{\mu}_t) \left(\frac{1}{\sigma} \frac{d\sigma}{d|\Delta\phi_{\ell+\ell-}|} \right)_{\text{NP}}. \quad (3)$$

The predicted shapes of the SM and NP terms in Eq. (3) are shown in Fig. 5. The NP term arises from interference with SM $t\bar{t}$ production, and therefore gives both positive and negative contributions to the differential cross section.

To set exclusion limits on $\text{Re}(\hat{\mu}_t)$, the SM and NP contributions to Eq. (3) are parametrized by polynomial functions (shown in Fig. 5), which are then used in a template fit to the measured normalized differential cross section. We use the projection in $|\Delta\phi_{\ell+\ell-}|$ of the measured normalized double-differential cross section in bins of $M_{t\bar{t}}$ to minimize the systematic uncertainty from top quark p_T modeling, as for the extraction of f_{SM} . The limits are derived under the

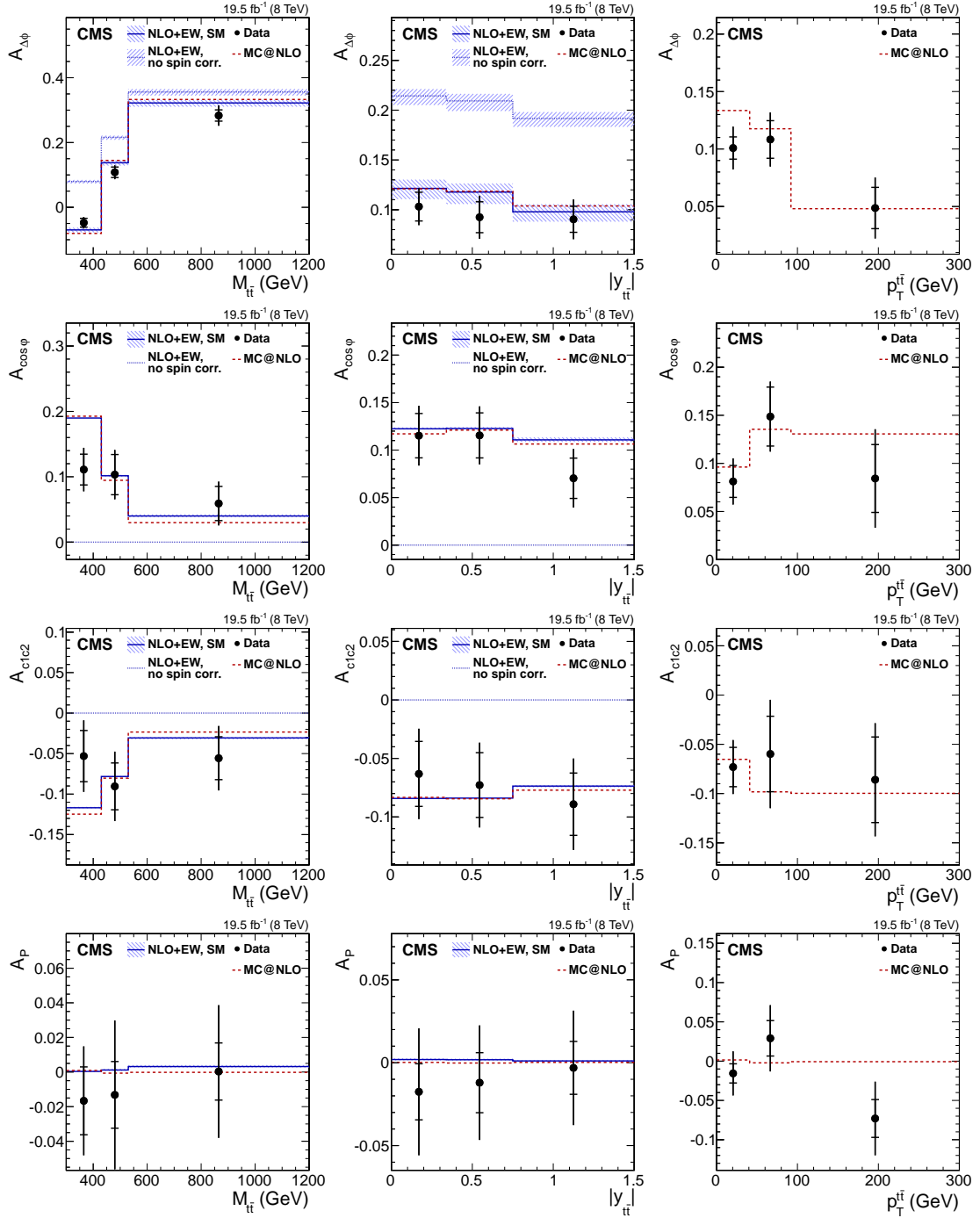


Figure 4: Dependence of the four asymmetry variables from data (points) on $M_{t\bar{t}}$ (left), $|y_{t\bar{t}}|$ (middle), and $p_T^{t\bar{t}}$ (right), obtained from the unfolded double-differential distributions; parton-level predictions from MC@NLO (dashed histograms); and theoretical predictions at NLO+EW [4, 62] with (SM) and without (no spin corr.) spin correlations (solid and dotted histograms, respectively). The inner and outer vertical bars on the data points represent the statistical and total uncertainties, respectively. The hatched bands represent variations of μ_R and μ_F simultaneously up and down by a factor of two. The last bin of each plot includes overflow events.

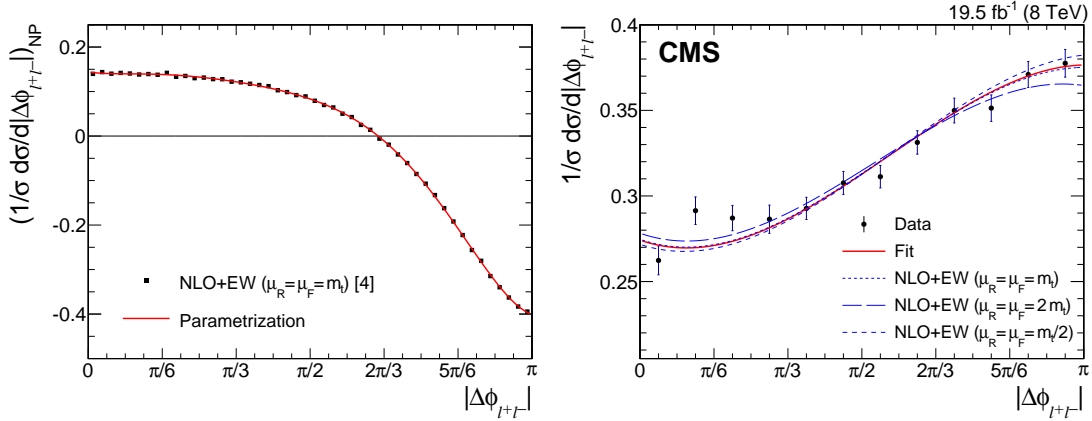


Figure 5: Left: theoretical prediction from Ref. [4] (points) and polynomial parametrization (line) for the contribution from new physics with a non-zero CMDM to the normalized differential cross section $(1/\sigma)(d\sigma/d|\Delta\phi_{\ell+\ell-}|)_{\text{NP}}$, for $\text{Re}(\hat{\mu}_t) \ll 1$. Right: normalized differential cross section from data (points). The solid line corresponds to the result of the fit to the form given in Eq. (3), and the dashed lines show the parametrized SM NLO+EW predictions for μ_R and μ_F equal to m_t , $2m_t$, and $m_t/2$. The vertical bars on the data points represent the total uncertainties.

assumption that the acceptance matrix is unchanged by the presence of NP. Studies of the effects of our selection criteria at the parton level show this leads to conservative limits. The fit is performed using a χ^2 minimization, accounting for both statistical and systematic uncertainties and their correlations, with $\text{Re}(\hat{\mu}_t)$ as the only free parameter. The systematic uncertainty arising from the choice of μ_R and μ_F in the theoretical calculations from Ref. [4] is estimated by repeating the fit after varying both scales together up and down by a factor of two. This constitutes the dominant source of uncertainty. The proper behavior of the fit is verified using pseudo-experiments. The result of the fit is $\text{Re}(\hat{\mu}_t) = -0.006 \pm 0.024$, and is shown graphically in Fig. 5. The corresponding 95% confidence level (CL) interval is $-0.053 < \text{Re}(\hat{\mu}_t) < 0.042$.

The spin correlation coefficient D is also sensitive to $\text{Re}(\hat{\mu}_t)$, and the CP-violating component of the top quark polarization P^{CPV} is sensitive to $\text{Im}(\hat{d}_t)$. Studies of the effects of our selection criteria at the parton level show that the presence of anomalous top quark chromo moments has no significant effect on the acceptance matrix for either of these variables, and we use this assumption in the derivation of limits on $\text{Re}(\hat{\mu}_t)$ and $\text{Im}(\hat{d}_t)$.

For the D coefficient, Eq. (3) simplifies to $D = D_{\text{SM}} + \text{Re}(\hat{\mu}_t) D_{\text{NP}}$ [4]. Using the values from Table 5, the relationship $D = -2A_{\cos\varphi}$, and taking $D_{\text{NP}} = -1.712 \pm 0.019$ from Ref. [4], we find $\text{Re}(\hat{\mu}_t) = -0.014 \pm 0.020$, with the corresponding 95% CL interval $-0.053 < \text{Re}(\hat{\mu}_t) < 0.026$. The constraints on $\text{Re}(\hat{\mu}_t)$ from D are stronger than those from the $|\Delta\phi_{\ell+\ell-}|$ fit because the smaller theoretical uncertainty in the SM NLO+EW calculation of D compared to that in the $|\Delta\phi_{\ell+\ell-}|$ distribution outweighs the slightly larger experimental uncertainty.

Similarly, P^{CPV} is related to $\text{Im}(\hat{d}_t)$ via $P^{\text{CPV}} = \text{Im}(\hat{d}_t) P_{\text{NP}}^{\text{CPV}}$, with $P_{\text{NP}}^{\text{CPV}} = 0.482 \pm 0.003$ [4]. We find $\text{Im}(\hat{d}_t) = -0.001 \pm 0.034$, with the corresponding 95% CL interval $-0.068 < \text{Im}(\hat{d}_t) < 0.067$.

The $|\Delta\phi_{\ell+\ell-}|$ distribution is potentially sensitive to pair-produced scalar top quark partners (top squarks) that decay to produce a top quark and antiquark with no additional visible particles. The spin-zero particles transmit no spin information from the initial state to the final-state top quarks, meaning such events look much like uncorrelated $t\bar{t}$ events. We assess the sensitiv-

ity of the measured $|\Delta\phi_{\ell^+\ell^-}|$ distribution to pair-produced top squarks with mass equal to m_t . As seen from the extracted value of f_{SM} in Table 6, the dominant source of uncertainty is the theoretical scale uncertainty in the $|\Delta\phi_{\ell^+\ell^-}|$ distribution. The result is that no exclusion limits on top squarks can be set using the $|\Delta\phi_{\ell^+\ell^-}|$ normalized differential cross section alone, and the additional sensitivity if combined with the inclusive measurement of the cross section is marginal.

9 Summary

Measurements of the $t\bar{t}$ spin correlations and the top quark polarization have been presented in the $t\bar{t}$ dilepton final states (e^+e^- , $e^\pm\mu^\mp$, and $\mu^+\mu^-$), using angular distributions unfolded to the parton level and as a function of the $t\bar{t}$ -system variables $M_{t\bar{t}}$, $|y_{t\bar{t}}|$, and $p_T^{t\bar{t}}$. The data sample corresponds to an integrated luminosity of 19.5 fb^{-1} from pp collisions at $\sqrt{s} = 8 \text{ TeV}$, collected by the CMS experiment at the LHC.

For the spin correlation coefficients, we measure $C_{\text{hel}} = 0.278 \pm 0.084$ and $D = 0.205 \pm 0.031$. The measurements sensitive to spin correlations are translated into determinations of f_{SM} , the strength of the spin correlations relative to the SM prediction. The most precise result comes from the measurement of $A_{\Delta\phi} = 0.095 \pm 0.006 \text{ (stat)} \pm 0.007 \text{ (syst)}$, yielding $f_{\text{SM}} = 1.12^{+0.12}_{-0.15}$. The SM (CP-conserving) top quark polarization is measured to be $P = -0.022 \pm 0.058$, while the CP-violating component is found to be $P^{\text{CPV}} = 0.000 \pm 0.016$. All measurements are in agreement with the SM expectations, and help constrain theories of physics beyond the SM.

The measured top quark spin observables are compared to theoretical predictions in order to search for hypothetical top quark anomalous couplings. No evidence of new physics is observed, and exclusion limits on the real part of the chromo-magnetic dipole moment $\text{Re}(\hat{\mu}_t)$ and the imaginary part of the chromo-electric dipole moment $\text{Im}(\hat{d}_t)$ are evaluated. Values outside the intervals $-0.053 < \text{Re}(\hat{\mu}_t) < 0.026$ and $-0.068 < \text{Im}(\hat{d}_t) < 0.067$ are excluded at the 95% confidence level, the first such measurements to date.

Acknowledgments

We would like to thank W. Bernreuther and Z.-G. Si for calculating the theoretical predictions for this paper, and for studies of the effect of anomalous top quark chromo moments on the acceptance of our selection criteria at the parton level. We congratulate our colleagues in the CERN accelerator departments for the excellent performance of the LHC and thank the technical and administrative staffs at CERN and at other CMS institutes for their contributions to the success of the CMS effort. In addition, we gratefully acknowledge the computing centres and personnel of the Worldwide LHC Computing Grid for delivering so effectively the computing infrastructure essential to our analyses. Finally, we acknowledge the enduring support for the construction and operation of the LHC and the CMS detector provided by the following funding agencies: the Austrian Federal Ministry of Science, Research and Economy and the Austrian Science Fund; the Belgian Fonds de la Recherche Scientifique, and Fonds voor Wetenschappelijk Onderzoek; the Brazilian Funding Agencies (CNPq, CAPES, FAPERJ, and FAPESP); the Bulgarian Ministry of Education and Science; CERN; the Chinese Academy of Sciences, Ministry of Science and Technology, and National Natural Science Foundation of China; the Colombian Funding Agency (COLCIENCIAS); the Croatian Ministry of Science, Education and Sport, and the Croatian Science Foundation; the Research Promotion Foundation, Cyprus; the Ministry of Education and Research, Estonian Research Council via IUT23-4 and

IUT23-6 and European Regional Development Fund, Estonia; the Academy of Finland, Finnish Ministry of Education and Culture, and Helsinki Institute of Physics; the Institut National de Physique Nucléaire et de Physique des Particules / CNRS, and Commissariat à l'Énergie Atomique et aux Énergies Alternatives / CEA, France; the Bundesministerium für Bildung und Forschung, Deutsche Forschungsgemeinschaft, and Helmholtz-Gemeinschaft Deutscher Forschungszentren, Germany; the General Secretariat for Research and Technology, Greece; the National Scientific Research Foundation, and National Innovation Office, Hungary; the Department of Atomic Energy and the Department of Science and Technology, India; the Institute for Studies in Theoretical Physics and Mathematics, Iran; the Science Foundation, Ireland; the Istituto Nazionale di Fisica Nucleare, Italy; the Ministry of Science, ICT and Future Planning, and National Research Foundation (NRF), Republic of Korea; the Lithuanian Academy of Sciences; the Ministry of Education, and University of Malaya (Malaysia); the Mexican Funding Agencies (CINVESTAV, CONACYT, SEP, and UASLP-FAI); the Ministry of Business, Innovation and Employment, New Zealand; the Pakistan Atomic Energy Commission; the Ministry of Science and Higher Education and the National Science Centre, Poland; the Fundação para a Ciência e a Tecnologia, Portugal; JINR, Dubna; the Ministry of Education and Science of the Russian Federation, the Federal Agency of Atomic Energy of the Russian Federation, Russian Academy of Sciences, and the Russian Foundation for Basic Research; the Ministry of Education, Science and Technological Development of Serbia; the Secretaría de Estado de Investigación, Desarrollo e Innovación and Programa Consolider-Ingenio 2010, Spain; the Swiss Funding Agencies (ETH Board, ETH Zurich, PSI, SNF, UniZH, Canton Zurich, and SER); the Ministry of Science and Technology, Taipei; the Thailand Center of Excellence in Physics, the Institute for the Promotion of Teaching Science and Technology of Thailand, Special Task Force for Activating Research and the National Science and Technology Development Agency of Thailand; the Scientific and Technical Research Council of Turkey, and Turkish Atomic Energy Authority; the National Academy of Sciences of Ukraine, and State Fund for Fundamental Researches, Ukraine; the Science and Technology Facilities Council, UK; the US Department of Energy, and the US National Science Foundation.

Individuals have received support from the Marie-Curie programme and the European Research Council and EPLANET (European Union); the Leventis Foundation; the A. P. Sloan Foundation; the Alexander von Humboldt Foundation; the Belgian Federal Science Policy Office; the Fonds pour la Formation à la Recherche dans l'Industrie et dans l'Agriculture (FRIA-Belgium); the Agentschap voor Innovatie door Wetenschap en Technologie (IWT-Belgium); the Ministry of Education, Youth and Sports (MEYS) of the Czech Republic; the Council of Science and Industrial Research, India; the HOMING PLUS programme of the Foundation for Polish Science, cofinanced from European Union, Regional Development Fund; the OPUS programme of the National Science Center (Poland); the Compagnia di San Paolo (Torino); MIUR project 20108T4XTM (Italy); the Thalís and Aristeia programmes cofinanced by EU-ESF and the Greek NSRF; the National Priorities Research Program by Qatar National Research Fund; the Rachadapisek Sompot Fund for Postdoctoral Fellowship, Chulalongkorn University (Thailand); the Chulalongkorn Academic into Its 2nd Century Project Advancement Project (Thailand); and the Welch Foundation, contract C-1845.

References

- [1] CMS Collaboration, "Measurement of the top quark mass using proton-proton data at $\sqrt{s} = 7$ and 8 TeV", (2015). [arXiv:1509.04044](#). Submitted to *Phys. Rev. D*.
- [2] D0 Collaboration, "Improved determination of the width of the top quark", *Phys. Rev. D* **85** (2012) 091104, [doi:10.1103/PhysRevD.85.091104](#), [arXiv:1201.4156](#).
- [3] G. Mahlon and S. J. Parke, "Spin correlation effects in top quark pair production at the LHC", *Phys. Rev. D* **81** (2010) 074024, [doi:10.1103/PhysRevD.81.074024](#), [arXiv:1001.3422](#).
- [4] W. Bernreuther and Z.-G. Si, "Top quark spin correlations and polarization at the LHC: standard model predictions and effects of anomalous top chromo moments", *Phys. Lett. B* **725** (2013) 115, [doi:10.1016/j.physletb.2013.06.051](#), [arXiv:1305.2066](#). [Erratum: *Phys. Lett. B* **744** (2015) 413].
- [5] D. Krohn, T. Liu, J. Shelton, and L.-T. Wang, "A polarized view of the top asymmetry", *Phys. Rev. D* **84** (2011) 074034, [doi:10.1103/PhysRevD.84.074034](#), [arXiv:1105.3743](#).
- [6] S. Fajfer, J. F. Kamenik, and B. Melic, "Discerning new physics in $t\bar{t}$ production using top spin observables at hadron colliders", *JHEP* **08** (2012) 114, [doi:10.1007/JHEP08\(2012\)114](#), [arXiv:1205.0264](#).
- [7] J. A. Aguilar-Saavedra and M. Perez-Victoria, " $t\bar{t}$ charge asymmetry, family and friends", *J. Phys.: Conf. Ser.* **447** [doi:10.1088/1742-6596/447/1/012015](#), [arXiv:1302.6618](#).
- [8] A. Brandenburg, Z.-G. Si, and P. Uwer, "QCD-corrected spin analysing power of jets in decays of polarized top quarks", *Phys. Lett. B* **539** (2002) 235, [doi:10.1016/S0370-2693\(02\)02098-1](#), [arXiv:hep-ph/0205023](#).
- [9] CDF Collaboration, "Measurement of $t\bar{t}$ spin correlation in $p\bar{p}$ collisions using the CDF II detector at the Tevatron", *Phys. Rev. D* **83** (2011) 031104, [doi:10.1103/PhysRevD.83.031104](#), [arXiv:1012.3093](#).
- [10] D0 Collaboration, "Evidence for spin correlation in $t\bar{t}$ production", *Phys. Rev. Lett.* **108** (2012) 032004, [doi:10.1103/PhysRevLett.108.032004](#), [arXiv:1110.4194](#).
- [11] D0 Collaboration, "Measurement of spin correlation in $t\bar{t}$ production using a matrix element approach", *Phys. Rev. Lett.* **107** (2011) 032001, [doi:10.1103/PhysRevLett.107.032001](#), [arXiv:1104.5194](#).
- [12] D0 Collaboration, "Measurement of leptonic asymmetries and top-quark polarization in $t\bar{t}$ production", *Phys. Rev. D* **87** (2013) 011103, [doi:10.1103/PhysRevD.87.011103](#), [arXiv:1207.0364](#).
- [13] ATLAS Collaboration, "Measurement of top quark polarization in top-antitop events from proton-proton collisions at $\sqrt{s} = 7$ TeV using the ATLAS detector", *Phys. Rev. Lett.* **111** (2013) 232002, [doi:10.1103/PhysRevLett.111.232002](#), [arXiv:1307.6511](#).
- [14] ATLAS Collaboration, "Measurement of spin correlation in top-antitop quark events and search for top squark pair production in pp collisions at $\sqrt{s} = 8$ TeV using the ATLAS detector", *Phys. Rev. Lett.* **114** (2015) 142001, [doi:10.1103/PhysRevLett.114.142001](#), [arXiv:1412.4742](#).

- [15] CMS Collaboration, “Measurements of $t\bar{t}$ spin correlations and top-quark polarization using dilepton final states in pp collisions at $\sqrt{s} = 7$ TeV”, *Phys. Rev. Lett.* **112** (2014) 182001, doi:10.1103/PhysRevLett.112.182001, arXiv:1311.3924.
- [16] CMS Collaboration, “The CMS experiment at the CERN LHC”, *JINST* **3** (2008) S08004, doi:10.1088/1748-0221/3/08/S08004.
- [17] CMS Collaboration, “Particle-flow event reconstruction in CMS and performance for jets, taus, and E_T^{miss} ”, CMS Physics Analysis Summary CMS-PAS-PFT-09-001, 2009.
- [18] CMS Collaboration, “Commissioning of the particle-flow event with the first LHC collisions recorded in the CMS detector”, CMS Physics Analysis Summary CMS-PAS-PFT-10-001, 2010.
- [19] CMS Collaboration, “Performance of electron reconstruction and selection with the CMS detector in proton-proton collisions at $\sqrt{s} = 8$ TeV”, *JINST* **10** (2015) P06005, doi:10.1088/1748-0221/10/06/P06005, arXiv:1502.02701.
- [20] CMS Collaboration, “Performance of CMS muon reconstruction in pp collision events at $\sqrt{s} = 7$ TeV”, *JINST* **7** (2012) P10002, doi:10.1088/1748-0221/7/10/P10002, arXiv:1206.4071.
- [21] CMS Collaboration, “Description and performance of track and primary-vertex reconstruction with the CMS tracker”, *JINST* **9** (2014) P10009, doi:10.1088/1748-0221/9/10/P10009, arXiv:1405.6569.
- [22] CMS Collaboration, “Search for top-squark pair production in the single-lepton final state in pp collisions at $\sqrt{s} = 8$ TeV”, *Eur. Phys. J. C* **73** (2013) 2677, doi:10.1140/epjc/s10052-013-2677-2, arXiv:1308.1586.
- [23] M. Cacciari, G. P. Salam, and G. Soyez, “The anti- k_t jet clustering algorithm”, *JHEP* **04** (2008) 063, doi:10.1088/1126-6708/2008/04/063, arXiv:0802.1189.
- [24] M. Cacciari, G. P. Salam, and G. Soyez, “FastJet user manual”, *Eur. Phys. J. C* **72** (2012) 1896, doi:10.1140/epjc/s10052-012-1896-2, arXiv:1111.6097.
- [25] M. Cacciari and G. P. Salam, “Pileup subtraction using jet areas”, *Phys. Lett. B* **659** (2008) 119, doi:10.1016/j.physletb.2007.09.077, arXiv:0707.1378.
- [26] CMS Collaboration, “Identification of b-quark jets with the CMS experiment”, *JINST* **8** (2013) P04013, doi:10.1088/1748-0221/8/04/P04013, arXiv:1211.4462.
- [27] S. Frixione and B. R. Webber, “Matching NLO QCD computations and parton shower simulations”, *JHEP* **06** (2002) doi:10.1088/1126-6708/2002/06/029, arXiv:hep-ph/0204244.
- [28] S. Frixione, P. Nason, and B. R. Webber, “Matching NLO QCD and parton showers in heavy flavor production”, *JHEP* **08** (2003) 007, doi:10.1088/1126-6708/2003/08/007, arXiv:hep-ph/0305252.
- [29] J. Pumplin et al., “New generation of parton distributions with uncertainties from global QCD analysis”, *JHEP* **07** (2002) 012, doi:10.1088/1126-6708/2002/07/012, arXiv:hep-ph/0201195.

- [30] G. Corcella et al., “HERWIG 6: an event generator for hadron emission reactions with interfering gluons (including supersymmetric processes)”, *JHEP* **01** (2001) 010, doi:10.1088/1126-6708/2001/01/010, arXiv:hep-ph/0011363.
- [31] J. Alwall et al., “MADGRAPH 5: going beyond”, *JHEP* **06** (2011) 128, doi:10.1007/JHEP06(2011)128, arXiv:1106.0522.
- [32] J. Alwall et al., “The automated computation of tree-level and next-to-leading order differential cross sections, and their matching to parton shower simulations”, *JHEP* **07** (2014) 079, doi:10.1007/JHEP07(2014)079, arXiv:1405.0301.
- [33] J. M. Campbell and R. K. Ellis, “MCFM for the Tevatron and the LHC”, *Nucl. Phys. Proc. Suppl.* **205-206** (2010) 10, doi:10.1016/j.nuclphysbps.2010.08.011, arXiv:1007.3492.
- [34] J. M. Campbell, R. K. Ellis, and C. Williams, “Vector boson pair production at the LHC”, *JHEP* **07** (2011) 018, doi:10.1007/JHEP07(2011)018, arXiv:1105.0020.
- [35] R. Frederix et al., “Four-lepton production at hadron colliders: aMC@NLO predictions with theoretical uncertainties”, *JHEP* **02** (2012) 099, doi:10.1007/JHEP02(2012)099, arXiv:1110.4738.
- [36] J. M. Campbell and R. K. Ellis, “ $t\bar{t}W^\pm$ production and decay at NLO”, *JHEP* **07** (2012) 052, doi:10.1007/JHEP07(2012)052, arXiv:1204.5678.
- [37] M. V. Garzelli, A. Kardos, C. G. Papadopoulos, and Z. Trocsanyi, “ $t\bar{t}W^\pm$ and $t\bar{t}Z$ hadroproduction at NLO accuracy in QCD with Parton Shower and Hadronization Effects”, *JHEP* **11** (2012) 056, doi:10.1007/JHEP11(2012)056, arXiv:1208.2665.
- [38] R. Gavin, Y. Li, F. Petriello, and S. Quackenbush, “W Physics at the LHC with FEWZ 2.1”, *Comput. Phys. Commun.* **184** (2013) 208, doi:10.1016/j.cpc.2012.09.005, arXiv:1201.5896.
- [39] P. Nason, “A new method for combining NLO QCD with shower Monte Carlo algorithms”, *JHEP* **11** (2004) 040, doi:10.1088/1126-6708/2004/11/040, arXiv:hep-ph/0409146.
- [40] S. Frixione, P. Nason, and C. Oleari, “Matching NLO QCD computations with parton shower simulations: the POWHEG method”, *JHEP* **11** (2007) 070, doi:10.1088/1126-6708/2007/11/070, arXiv:0709.2092.
- [41] S. Alioli, P. Nason, C. Oleari, and E. Re, “A general framework for implementing NLO calculations in shower Monte Carlo programs: the POWHEG BOX”, *JHEP* **06** (2010) 043, doi:10.1007/JHEP06(2010)043, arXiv:1002.2581.
- [42] N. Kidonakis, “Next-to-next-to-leading-order collinear and soft gluon corrections for t -channel single top quark production”, *Phys. Rev. D* **83** (2011) 091503, doi:10.1103/PhysRevD.83.091503, arXiv:1103.2792.
- [43] N. Kidonakis, “NNLL resummation for s -channel single top quark production”, *Phys. Rev. D* **81** (2010) 054028, doi:10.1103/PhysRevD.81.054028, arXiv:1001.5034.
- [44] S. Alioli, P. Nason, C. Oleari, and E. Re, “NLO single-top production matched with shower in POWHEG: s - and t -channel contributions”, *JHEP* **09** (2009) 111, doi:10.1088/1126-6708/2009/09/111, arXiv:0907.4076. [Erratum: doi:10.1007/JHEP02(2010)011].

- [45] N. Kidonakis, “Two-loop soft anomalous dimensions for single top quark associated production with a W^- or H^- ”, *Phys. Rev. D* **82** (2010) 054018, doi:10.1103/PhysRevD.82.054018, arXiv:1005.4451.
- [46] E. Re, “Single-top tW -channel production matched with parton showers using the POWHEG method”, *Eur. Phys. J. C* **71** (2011) 1547, doi:10.1140/epjc/s10052-011-1547-z, arXiv:1009.2450.
- [47] T. Sjöstrand, S. Mrenna, and P. Skands, “PYTHIA 6.4 physics and manual”, *JHEP* **05** (2006) 026, doi:10.1088/1126-6708/2006/05/026, arXiv:0706.2334.
- [48] GEANT4 Collaboration, “GEANT4—a simulation toolkit”, *Nucl. Instrum. Meth. A* **506** (2003) 250, doi:10.1016/S0168-9002(03)01368-8.
- [49] CMS Collaboration, “Observation of the associated production of a single top quark and a W boson in pp collisions at $\sqrt{s} = 8$ TeV”, *Phys. Rev. Lett.* **112** (2014) 231802, doi:10.1103/PhysRevLett.112.231802, arXiv:1401.2942.
- [50] CMS Collaboration, “Measurement of the sum of WW and WZ production with W +dijet events in pp collisions at $\sqrt{s} = 7$ TeV”, *Eur. Phys. J. C* **73** (2013) 2283, doi:10.1140/epjc/s10052-013-2283-3, arXiv:1210.7544.
- [51] CMS Collaboration, “Measurement of WZ and ZZ production in pp collisions at $\sqrt{s} = 8$ TeV in final states with b -tagged jets”, *Eur. Phys. J. C* **74** (2014) 2973, doi:10.1140/epjc/s10052-014-2973-5, arXiv:1403.3047.
- [52] CMS Collaboration, “Observation of top quark pairs produced in association with a vector boson in pp collisions at $\sqrt{s} = 8$ TeV”, (2015). arXiv:1510.01131. Submitted to JHEP.
- [53] B. A. Betchart, R. Demina, and A. Harel, “Analytic solutions for neutrino momenta in decay of top quarks”, *Nucl. Instrum. Meth. A* **736** (2014) 169, doi:10.1016/j.nima.2013.10.039, arXiv:1305.1878.
- [54] CMS Collaboration, “Measurement of the $t\bar{t}$ production cross section and the top quark mass in the dilepton channel in pp collisions at $\sqrt{s} = 7$ TeV”, *JHEP* **07** (2011) 049, doi:10.1007/JHEP07(2011)049, arXiv:1105.5661.
- [55] S. Schmitt, “TUnfold, an algorithm for correcting migration effects in high energy physics”, *JINST* **7** (2012) P10003, doi:10.1088/1748-0221/7/10/T10003, arXiv:1205.6201.
- [56] CMS Collaboration, “Determination of jet energy calibration and transverse momentum resolution in CMS”, *JINST* **6** (2011) P11002, doi:10.1088/1748-0221/6/11/P11002, arXiv:1107.4277.
- [57] CMS Collaboration, “Energy calibration and resolution of the CMS electromagnetic calorimeter in pp collisions at $\sqrt{s} = 7$ TeV”, *JINST* **8** (2013) doi:10.1088/1748-0221/8/09/P09009, arXiv:1306.2016.
- [58] S. Alekhin et al., “The PDF4LHC Working Group interim report”, (2011). arXiv:1101.0536.
- [59] M. Botje et al., “The PDF4LHC Working Group interim recommendations”, (2011). arXiv:1101.0538.

-
- [60] CMS Collaboration, “Measurement of differential top-quark pair production cross sections in pp collisions at $\sqrt{s} = 7$ TeV”, *Eur. Phys. J. C* **73** (2013) 2339, doi:10.1140/epjc/s10052-013-2339-4, arXiv:1211.2220.
- [61] CMS Collaboration, “Measurement of the differential cross section for top quark pair production in pp collisions at $\sqrt{s} = 8$ TeV”, *Eur. Phys. J. C* **75** (2015) 542, doi:10.1140/epjc/s10052-015-3709-x, arXiv:1505.04480.
- [62] W. Bernreuther and Z.-G. Si, “Distributions and correlations for top quark pair production and decay at the Tevatron and LHC”, *Nucl. Phys. B* **837** (2010) 90, doi:10.1016/j.nuclphysb.2010.05.001, arXiv:1003.3926.

10 The CMS Collaboration

Yerevan Physics Institute, Yerevan, Armenia

V. Khachatryan, A.M. Sirunyan, A. Tumasyan

Institut für Hochenergiephysik der OeAW, Wien, Austria

W. Adam, E. Asilar, T. Bergauer, J. Brandstetter, E. Brondolin, M. Dragicevic, J. Erö, M. Flechl, M. Friedl, R. Frühwirth¹, V.M. Ghete, C. Hartl, N. Hörmann, J. Hrubec, M. Jeitler¹, V. Knünz, A. König, M. Krammer¹, I. Krätschmer, D. Liko, T. Matsushita, I. Mikulec, D. Rabadý², N. Rad, B. Rahbaran, H. Rohringer, J. Schieck¹, R. Schöfbeck, J. Strauss, W. Treberer-Treberspurg, W. Waltenberger, C.-E. Wulz¹

National Centre for Particle and High Energy Physics, Minsk, Belarus

V. Mossolov, N. Shumeiko, J. Suarez Gonzalez

Universiteit Antwerpen, Antwerpen, Belgium

S. Alderweireldt, T. Cornelis, E.A. De Wolf, X. Janssen, A. Knutsson, J. Lauwers, S. Luyckx, M. Van De Klundert, H. Van Haevermaet, P. Van Mechelen, N. Van Remortel, A. Van Spilbeeck

Vrije Universiteit Brussel, Brussel, Belgium

S. Abu Zeid, F. Blekman, J. D'Hondt, N. Daci, I. De Bruyn, K. Deroover, N. Heracleous, J. Keaveney, S. Lowette, L. Moreels, A. Olbrechts, Q. Python, D. Strom, S. Tavernier, W. Van Doninck, P. Van Mulders, G.P. Van Onsem, I. Van Parijs

Université Libre de Bruxelles, Bruxelles, Belgium

P. Barria, H. Brun, C. Caillol, B. Clerboux, G. De Lentdecker, W. Fang, G. Fasanella, L. Favart, R. Goldouzian, A. Grebenyuk, G. Karapostoli, T. Lenzi, A. Léonard, T. Maerschalk, A. Marinov, L. Perniè, A. Randle-conde, T. Seva, C. Vander Velde, P. Vanlaer, R. Yonamine, F. Zenoni, F. Zhang³

Ghent University, Ghent, Belgium

K. Beernaert, L. Benucci, A. Cimmino, S. Crucy, D. Dobur, A. Fagot, G. Garcia, M. Gul, J. Mccartin, A.A. Ocampo Rios, D. Poyraz, D. Ryckbosch, S. Salva, M. Sigamani, M. Tytgat, W. Van Driessche, E. Yazgan, N. Zaganidis

Université Catholique de Louvain, Louvain-la-Neuve, Belgium

S. Basegmez, C. Beluffi⁴, O. Bondu, S. Brochet, G. Bruno, A. Caudron, L. Ceard, C. Delaere, D. Favart, L. Forthomme, A. Giammanco⁵, A. Jafari, P. Jez, M. Komm, V. Lemaitre, A. Mertens, M. Musich, C. Nuttens, L. Perrini, K. Piotrkowski, A. Popov⁶, L. Quertenmont, M. Selvaggi, M. Vidal Marono

Université de Mons, Mons, Belgium

N. Belyi, G.H. Hammad

Centro Brasileiro de Pesquisas Fisicas, Rio de Janeiro, Brazil

W.L. Aldá Júnior, F.L. Alves, G.A. Alves, L. Brito, M. Correa Martins Junior, M. Hamer, C. Hensel, A. Moraes, M.E. Pol, P. Rebello Teles

Universidade do Estado do Rio de Janeiro, Rio de Janeiro, Brazil

E. Belchior Batista Das Chagas, W. Carvalho, J. Chinellato⁷, A. Custódio, E.M. Da Costa, D. De Jesus Damiao, C. De Oliveira Martins, S. Fonseca De Souza, L.M. Huertas Guativa, H. Malbouisson, D. Matos Figueiredo, C. Mora Herrera, L. Mundim, H. Nogima, W.L. Prado Da Silva, A. Santoro, A. Sznajder, E.J. Tonelli Manganote⁷, A. Vilela Pereira

Universidade Estadual Paulista ^a, Universidade Federal do ABC ^b, São Paulo, Brazil

S. Ahuja^a, C.A. Bernardes^b, A. De Souza Santos^b, S. Dogra^a, T.R. Fernandez Perez Tomei^a, E.M. Gregores^b, P.G. Mercadante^b, C.S. Moon^{a,8}, S.F. Novaes^a, Sandra S. Padula^a, D. Romero Abad, J.C. Ruiz Vargas

Institute for Nuclear Research and Nuclear Energy, Sofia, Bulgaria

A. Aleksandrov, R. Hadjiiska, P. Iaydjiev, M. Rodozov, S. Stoykova, G. Sultanov, M. Vutova

University of Sofia, Sofia, Bulgaria

A. Dimitrov, I. Glushkov, L. Litov, B. Pavlov, P. Petkov

Institute of High Energy Physics, Beijing, China

M. Ahmad, J.G. Bian, G.M. Chen, H.S. Chen, M. Chen, T. Cheng, R. Du, C.H. Jiang, D. Leggat, R. Plestina⁹, F. Romeo, S.M. Shaheen, A. Spiezia, J. Tao, C. Wang, Z. Wang, H. Zhang

State Key Laboratory of Nuclear Physics and Technology, Peking University, Beijing, China

C. Asawatrangkuldee, Y. Ban, Q. Li, S. Liu, Y. Mao, S.J. Qian, D. Wang, Z. Xu

Universidad de Los Andes, Bogota, Colombia

C. Avila, A. Cabrera, L.F. Chaparro Sierra, C. Florez, J.P. Gomez, B. Gomez Moreno, J.C. Sanabria

University of Split, Faculty of Electrical Engineering, Mechanical Engineering and Naval Architecture, Split, Croatia

N. Godinovic, D. Lelas, I. Puljak, P.M. Ribeiro Cipriano

University of Split, Faculty of Science, Split, Croatia

Z. Antunovic, M. Kovac

Institute Rudjer Boskovic, Zagreb, Croatia

V. Brigljevic, K. Kadija, J. Luetic, S. Micanovic, L. Sudic

University of Cyprus, Nicosia, Cyprus

A. Attikis, G. Mavromanolakis, J. Mousa, C. Nicolaou, F. Ptochos, P.A. Razis, H. Rykaczewski

Charles University, Prague, Czech Republic

M. Bodlak, M. Finger¹⁰, M. Finger Jr.¹⁰

Academy of Scientific Research and Technology of the Arab Republic of Egypt, Egyptian Network of High Energy Physics, Cairo, Egypt

A.A. Abdelalim^{11,12}, A. Awad, A. Mahrous¹¹, A. Radi^{13,14}

National Institute of Chemical Physics and Biophysics, Tallinn, Estonia

B. Calpas, M. Kadastik, M. Murumaa, M. Raidal, A. Tiko, C. Veelken

Department of Physics, University of Helsinki, Helsinki, Finland

P. Eerola, J. Pekkanen, M. Voutilainen

Helsinki Institute of Physics, Helsinki, Finland

J. Härkönen, V. Karimäki, R. Kinnunen, T. Lampén, K. Lassila-Perini, S. Lehti, T. Lindén, P. Luukka, T. Peltola, J. Tuominiemi, E. Tuovinen, L. Wendland

Lappeenranta University of Technology, Lappeenranta, Finland

J. Talvitie, T. Tuuva

DSM/IRFU, CEA/Saclay, Gif-sur-Yvette, France

M. Besancon, F. Couderc, M. Dejardin, D. Denegri, B. Fabbro, J.L. Faure, C. Favaro, F. Ferri,

S. Ganjour, A. Givernaud, P. Gras, G. Hamel de Monchenault, P. Jarry, E. Locci, M. Machet, J. Malcles, J. Rander, A. Rosowsky, M. Titov, A. Zghiche

Laboratoire Leprince-Ringuet, Ecole Polytechnique, IN2P3-CNRS, Palaiseau, France

I. Antropov, S. Baffioni, F. Beaudette, P. Busson, L. Cadamuro, E. Chapon, C. Charlot, O. Davignon, N. Filipovic, R. Granier de Cassagnac, M. Jo, S. Lisniak, L. Mastrolorenzo, P. Miné, I.N. Naranjo, M. Nguyen, C. Ochando, G. Ortona, P. Paganini, P. Pigard, S. Regnard, R. Salerno, J.B. Sauvan, Y. Sirois, T. Strebler, Y. Yilmaz, A. Zabi

Institut Pluridisciplinaire Hubert Curien, Université de Strasbourg, Université de Haute Alsace Mulhouse, CNRS/IN2P3, Strasbourg, France

J.-L. Agram¹⁵, J. Andrea, A. Aubin, D. Bloch, J.-M. Brom, M. Buttignol, E.C. Chabert, N. Chanon, C. Collard, E. Conte¹⁵, X. Coubez, J.-C. Fontaine¹⁵, D. Gelé, U. Goerlach, C. Goetzmann, A.-C. Le Bihan, J.A. Merlin², K. Skovpen, P. Van Hove

Centre de Calcul de l'Institut National de Physique Nucleaire et de Physique des Particules, CNRS/IN2P3, Villeurbanne, France

S. Gadrat

Université de Lyon, Université Claude Bernard Lyon 1, CNRS-IN2P3, Institut de Physique Nucléaire de Lyon, Villeurbanne, France

S. Beauceron, C. Bernet, G. Boudoul, E. Bouvier, C.A. Carrillo Montoya, R. Chierici, D. Contardo, B. Courbon, P. Depasse, H. El Mamouni, J. Fan, J. Fay, S. Gascon, M. Gouzevitch, B. Ille, F. Lagarde, I.B. Laktineh, M. Lethuillier, L. Mirabito, A.L. Pequegnot, S. Perries, J.D. Ruiz Alvarez, D. Sabes, L. Sgandurra, V. Sordini, M. Vander Donckt, P. Verdier, S. Viret

Georgian Technical University, Tbilisi, Georgia

T. Toriashvili¹⁶

Tbilisi State University, Tbilisi, Georgia

D. Lomidze

RWTH Aachen University, I. Physikalisches Institut, Aachen, Germany

C. Autermann, S. Beranek, L. Feld, A. Heister, M.K. Kiesel, K. Klein, M. Lipinski, A. Ostapchuk, M. Preuten, F. Raupach, S. Schael, J.F. Schulte, T. Verlage, H. Weber, V. Zhukov⁶

RWTH Aachen University, III. Physikalisches Institut A, Aachen, Germany

M. Ata, M. Brodski, E. Dietz-Laursonn, D. Duchardt, M. Endres, M. Erdmann, S. Erdweg, T. Esch, R. Fischer, A. Güth, T. Hebbeker, C. Heidemann, K. Hoepfner, S. Knutzen, P. Kreuzer, M. Merschmeyer, A. Meyer, P. Millet, S. Mukherjee, M. Olschewski, K. Padeken, P. Papacz, T. Pook, M. Radziej, H. Reithler, M. Rieger, F. Scheuch, L. Sonnenschein, D. Teyssier, S. Thüer

RWTH Aachen University, III. Physikalisches Institut B, Aachen, Germany

V. Cherepanov, Y. Erdogan, G. Flügge, H. Geenen, M. Geisler, F. Hoehle, B. Kargoll, T. Kress, A. Künsken, J. Lingemann, A. Nehrkorn, A. Nowack, I.M. Nugent, C. Pistone, O. Pooth, A. Stahl

Deutsches Elektronen-Synchrotron, Hamburg, Germany

M. Aldaya Martin, I. Asin, N. Bartosik, O. Behnke, U. Behrens, K. Borras¹⁷, A. Burgmeier, A. Campbell, C. Contreras-Campana, F. Costanza, C. Diez Pardos, G. Dolinska, S. Dooling, T. Dorland, G. Eckerlin, D. Eckstein, T. Eichhorn, G. Flucke, E. Gallo¹⁸, J. Garay Garcia, A. Geiser, A. Gizhko, P. Gunnellini, J. Hauk, M. Hempel¹⁹, H. Jung, A. Kalogeropoulos, O. Karacheban¹⁹, M. Kasemann, P. Katsas, J. Kieseler, C. Kleinwort, I. Korol, W. Lange, J. Leonard, K. Lipka, A. Lobanov, W. Lohmann¹⁹, R. Mankel, I.-A. Melzer-Pellmann,

A.B. Meyer, G. Mittag, J. Mnich, A. Mussgiller, S. Naumann-Emme, A. Nayak, E. Ntomari, H. Perrey, D. Pitzl, R. Placakyte, A. Raspereza, B. Roland, M.Ö. Sahin, P. Saxena, T. Schoerner-Sadenius, C. Seitz, S. Spannagel, N. Stefaniuk, K.D. Trippkewitz, R. Walsh, C. Wissing

University of Hamburg, Hamburg, Germany

V. Blobel, M. Centis Vignali, A.R. Draeger, J. Erfle, E. Garutti, K. Goebel, D. Gonzalez, M. Görner, J. Haller, M. Hoffmann, R.S. Höing, A. Junkes, R. Klanner, R. Kogler, N. Kovalchuk, T. Lapsien, T. Lenz, I. Marchesini, D. Marconi, M. Meyer, D. Nowatschin, J. Ott, F. Pantaleo², T. Peiffer, A. Perieanu, N. Pietsch, J. Poehlsen, D. Rathjens, C. Sander, C. Scharf, P. Schleper, E. Schlieckau, A. Schmidt, S. Schumann, J. Schwandt, V. Sola, H. Stadie, G. Steinbrück, F.M. Stober, H. Tholen, D. Troendle, E. Usai, L. Vanelderen, A. Vanhoefer, B. Vormwald

Institut für Experimentelle Kernphysik, Karlsruhe, Germany

C. Barth, C. Baus, J. Berger, C. Böser, E. Butz, T. Chwalek, F. Colombo, W. De Boer, A. Descroix, A. Dierlamm, S. Fink, F. Frensch, R. Friese, M. Giffels, A. Gilbert, D. Haitz, F. Hartmann², S.M. Heindl, U. Husemann, I. Katkov⁶, A. Kornmayer², P. Lobelle Pardo, B. Maier, H. Mildner, M.U. Mozer, T. Müller, Th. Müller, M. Plagge, G. Quast, K. Rabbertz, S. Röcker, F. Roscher, M. Schröder, G. Sieber, H.J. Simonis, R. Ulrich, J. Wagner-Kuhr, S. Wayand, M. Weber, T. Weiler, S. Williamson, C. Wöhrmann, R. Wolf

Institute of Nuclear and Particle Physics (INPP), NCSR Demokritos, Aghia Paraskevi, Greece

G. Anagnostou, G. Daskalakis, T. Gerasis, V.A. Giakoumopoulou, A. Kyriakis, D. Loukas, A. Psallidas, I. Topsis-Giotis

National and Kapodistrian University of Athens, Athens, Greece

A. Agapitos, S. Kesisoglou, A. Panagiotou, N. Saoulidou, E. Tziaferi

University of Ioánnina, Ioánnina, Greece

I. Evangelou, G. Flouris, C. Foudas, P. Kokkas, N. Loukas, N. Manthos, I. Papadopoulos, E. Paradas, J. Strologas

Wigner Research Centre for Physics, Budapest, Hungary

G. Bencze, C. Hajdu, A. Hazi, P. Hidas, D. Horvath²⁰, F. Sikler, V. Veszpremi, G. Vesztergombi²¹, A.J. Zsigmond

Institute of Nuclear Research ATOMKI, Debrecen, Hungary

N. Beni, S. Czellar, J. Karancsi²², J. Molnar, Z. Szillasi²

University of Debrecen, Debrecen, Hungary

M. Bartók²³, A. Makovec, P. Raics, Z.L. Trocsanyi, B. Ujvari

National Institute of Science Education and Research, Bhubaneswar, India

S. Choudhury²⁴, P. Mal, K. Mandal, D.K. Sahoo, N. Sahoo, S.K. Swain

Panjab University, Chandigarh, India

S. Bansal, S.B. Beri, V. Bhatnagar, R. Chawla, R. Gupta, U. Bhawandeep, A.K. Kalsi, A. Kaur, M. Kaur, R. Kumar, A. Mehta, M. Mittal, J.B. Singh, G. Walia

University of Delhi, Delhi, India

Ashok Kumar, A. Bhardwaj, B.C. Choudhary, R.B. Garg, S. Malhotra, M. Naimuddin, N. Nishu, K. Ranjan, R. Sharma, V. Sharma

Saha Institute of Nuclear Physics, Kolkata, India

S. Bhattacharya, K. Chatterjee, S. Dey, S. Dutta, N. Majumdar, A. Modak, K. Mondal, S. Mukhopadhyay, A. Roy, D. Roy, S. Roy Chowdhury, S. Sarkar, M. Sharan

Bhabha Atomic Research Centre, Mumbai, India

A. Abdulsalam, R. Chudasama, D. Dutta, V. Jha, V. Kumar, A.K. Mohanty², L.M. Pant, P. Shukla, A. Topkar

Tata Institute of Fundamental Research, Mumbai, India

T. Aziz, S. Banerjee, S. Bhowmik²⁵, R.M. Chatterjee, R.K. Dewanjee, S. Dugad, S. Ganguly, S. Ghosh, M. Guchait, A. Gurtu²⁶, Sa. Jain, G. Kole, S. Kumar, B. Mahakud, M. Maity²⁵, G. Majumder, K. Mazumdar, S. Mitra, G.B. Mohanty, B. Parida, T. Sarkar²⁵, N. Sur, B. Sutar, N. Wickramage²⁷

Indian Institute of Science Education and Research (IISER), Pune, India

S. Chauhan, S. Dube, A. Kapoor, K. Kothekar, S. Sharma

Institute for Research in Fundamental Sciences (IPM), Tehran, Iran

H. Bakhshiansohi, H. Behnamian, S.M. Etesami²⁸, A. Fahim²⁹, M. Khakzad, M. Mohammadi Najafabadi, M. Naseri, S. Paktinat Mehdiabadi, F. Rezaei Hosseinabadi, B. Safarzadeh³⁰, M. Zeinali

University College Dublin, Dublin, Ireland

M. Felcini, M. Grunewald

INFN Sezione di Bari ^a, Università di Bari ^b, Politecnico di Bari ^c, Bari, Italy

M. Abbrescia^{a,b}, C. Calabria^{a,b}, C. Caputo^{a,b}, A. Colaleo^a, D. Creanza^{a,c}, L. Cristella^{a,b}, N. De Filippis^{a,c}, M. De Palma^{a,b}, L. Fiore^a, G. Iaselli^{a,c}, G. Maggi^{a,c}, M. Maggi^a, G. Miniello^{a,b}, S. My^{a,c}, S. Nuzzo^{a,b}, A. Pompili^{a,b}, G. Pugliese^{a,c}, R. Radogna^{a,b}, A. Ranieri^a, G. Selvaggi^{a,b}, L. Silvestris^{a,2}, R. Venditti^{a,b}

INFN Sezione di Bologna ^a, Università di Bologna ^b, Bologna, Italy

G. Abbiendi^a, C. Battilana², D. Bonacorsi^{a,b}, S. Braibant-Giacomelli^{a,b}, L. Brigliadori^{a,b}, R. Campanini^{a,b}, P. Capiluppi^{a,b}, A. Castro^{a,b}, F.R. Cavallo^a, S.S. Chhibra^{a,b}, G. Codispoti^{a,b}, M. Cuffiani^{a,b}, G.M. Dallavalle^a, F. Fabbri^a, A. Fanfani^{a,b}, D. Fasanella^{a,b}, P. Giacomelli^a, C. Grandi^a, L. Guiducci^{a,b}, S. Marcellini^a, G. Masetti^a, A. Montanari^a, F.L. Navarria^{a,b}, A. Perrotta^a, A.M. Rossi^{a,b}, T. Rovelli^{a,b}, G.P. Siroli^{a,b}, N. Tosi^{a,b,2}

INFN Sezione di Catania ^a, Università di Catania ^b, Catania, Italy

G. Cappello^b, M. Chiorboli^{a,b}, S. Costa^{a,b}, A. Di Mattia^a, F. Giordano^{a,b}, R. Potenza^{a,b}, A. Tricomi^{a,b}, C. Tuve^{a,b}

INFN Sezione di Firenze ^a, Università di Firenze ^b, Firenze, Italy

G. Barbagli^a, V. Ciulli^{a,b}, C. Civinini^a, R. D'Alessandro^{a,b}, E. Focardi^{a,b}, V. Gori^{a,b}, P. Lenzi^{a,b}, M. Meschini^a, S. Paoletti^a, G. Sguazzoni^a, L. Viliani^{a,b,2}

INFN Laboratori Nazionali di Frascati, Frascati, Italy

L. Benussi, S. Bianco, F. Fabbri, D. Piccolo, F. Primavera²

INFN Sezione di Genova ^a, Università di Genova ^b, Genova, Italy

V. Calvelli^{a,b}, F. Ferro^a, M. Lo Vetere^{a,b}, M.R. Monge^{a,b}, E. Robutti^a, S. Tosi^{a,b}

INFN Sezione di Milano-Bicocca ^a, Università di Milano-Bicocca ^b, Milano, Italy

L. Brianza, M.E. Dinardo^{a,b}, S. Fiorendi^{a,b}, S. Gennai^a, R. Gerosa^{a,b}, A. Ghezzi^{a,b}, P. Govoni^{a,b},

S. Malvezzi^a, R.A. Manzoni^{a,b,2}, B. Marzocchi^{a,b}, D. Menasce^a, L. Moroni^a, M. Paganoni^{a,b}, D. Pedrini^a, S. Ragazzi^{a,b}, N. Redaelli^a, T. Tabarelli de Fatis^{a,b}

INFN Sezione di Napoli^a, Università di Napoli 'Federico II'^b, Napoli, Italy, Università della Basilicata^c, Potenza, Italy, Università G. Marconi^d, Roma, Italy

S. Buontempo^a, N. Cavallo^{a,c}, S. Di Guida^{a,d,2}, M. Esposito^{a,b}, F. Fabozzi^{a,c}, A.O.M. Iorio^{a,b}, G. Lanza^a, L. Lista^a, S. Meola^{a,d,2}, M. Merola^a, P. Paolucci^{a,2}, C. Sciacca^{a,b}, F. Thyssen

INFN Sezione di Padova^a, Università di Padova^b, Padova, Italy, Università di Trento^c, Trento, Italy

P. Azzi^{a,2}, N. Bacchetta^a, L. Benato^{a,b}, D. Bisello^{a,b}, A. Boletti^{a,b}, A. Branca^{a,b}, R. Carlin^{a,b}, P. Checchia^a, M. Dall'Osso^{a,b,2}, T. Dorigo^a, U. Dosselli^a, F. Fanzago^a, F. Gasparini^{a,b}, U. Gasparini^{a,b}, A. Gozzelino^a, K. Kanishchev^{a,c}, S. Lacaprara^a, M. Margoni^{a,b}, A.T. Meneguzzo^{a,b}, J. Pazzini^{a,b,2}, N. Pozzobon^{a,b}, P. Ronchese^{a,b}, F. Simonetto^{a,b}, E. Torassa^a, M. Tosi^{a,b}, M. Zanetti, P. Zotto^{a,b}, A. Zucchetta^{a,b,2}, G. Zumerle^{a,b}

INFN Sezione di Pavia^a, Università di Pavia^b, Pavia, Italy

A. Braghieri^a, A. Magnani^{a,b}, P. Montagna^{a,b}, S.P. Ratti^{a,b}, V. Re^a, C. Riccardi^{a,b}, P. Salvini^a, I. Vai^{a,b}, P. Vitulo^{a,b}

INFN Sezione di Perugia^a, Università di Perugia^b, Perugia, Italy

L. Alunni Solestizi^{a,b}, G.M. Bilei^a, D. Ciangottini^{a,b,2}, L. Fanò^{a,b}, P. Lariccia^{a,b}, G. Mantovani^{a,b}, M. Menichelli^a, A. Saha^a, A. Santocchia^{a,b}

INFN Sezione di Pisa^a, Università di Pisa^b, Scuola Normale Superiore di Pisa^c, Pisa, Italy

K. Androsov^{a,31}, P. Azzurri^{a,2}, G. Bagliesi^a, J. Bernardini^a, T. Boccali^a, R. Castaldi^a, M.A. Ciocci^{a,31}, R. Dell'Orso^a, S. Donato^{a,c,2}, G. Fedi, L. Foà^{a,c†}, A. Giassi^a, M.T. Grippo^{a,31}, F. Ligabue^{a,c}, T. Lomtadze^a, L. Martini^{a,b}, A. Messineo^{a,b}, F. Palla^a, A. Rizzi^{a,b}, A. Savoy-Navarro^{a,32}, A.T. Serban^a, P. Spagnolo^a, R. Tenchini^a, G. Tonelli^{a,b}, A. Venturi^a, P.G. Verdini^a

INFN Sezione di Roma^a, Università di Roma^b, Roma, Italy

L. Barone^{a,b}, F. Cavallari^a, G. D'imperio^{a,b,2}, D. Del Re^{a,b,2}, M. Diemoz^a, S. Gelli^{a,b}, C. Jorda^a, E. Longo^{a,b}, F. Margaroli^{a,b}, P. Meridiani^a, G. Organtini^{a,b}, R. Paramatti^a, F. Preiato^{a,b}, S. Rahatlou^{a,b}, C. Rovelli^a, F. Santanastasio^{a,b}, P. Traczyk^{a,b,2}

INFN Sezione di Torino^a, Università di Torino^b, Torino, Italy, Università del Piemonte Orientale^c, Novara, Italy

N. Amapane^{a,b}, R. Arcidiacono^{a,c,2}, S. Argiro^{a,b}, M. Arneodo^{a,c}, R. Bellan^{a,b}, C. Biino^a, N. Cartiglia^a, M. Costa^{a,b}, R. Covarelli^{a,b}, A. Degano^{a,b}, N. Demaria^a, L. Finco^{a,b,2}, B. Kiani^{a,b}, C. Mariotti^a, S. Maselli^a, E. Migliore^{a,b}, V. Monaco^{a,b}, E. Monteil^{a,b}, M.M. Obertino^{a,b}, L. Pacher^{a,b}, N. Pastrone^a, M. Pelliccioni^a, G.L. Pinna Angioni^{a,b}, F. Ravera^{a,b}, A. Romero^{a,b}, M. Ruspa^{a,c}, R. Sacchi^{a,b}, A. Solano^{a,b}, A. Staiano^a

INFN Sezione di Trieste^a, Università di Trieste^b, Trieste, Italy

S. Belforte^a, V. Candelise^{a,b}, M. Casarsa^a, F. Cossutti^a, G. Della Ricca^{a,b}, B. Gobbo^a, C. La Licata^{a,b}, M. Marone^{a,b}, A. Schizzi^{a,b}, A. Zanetti^a

Kangwon National University, Chunchon, Korea

A. Kropivnitskaya, S.K. Nam

Kyungpook National University, Daegu, Korea

D.H. Kim, G.N. Kim, M.S. Kim, D.J. Kong, S. Lee, Y.D. Oh, A. Sakharov, D.C. Son

Chonbuk National University, Jeonju, Korea

J.A. Brochero Cifuentes, H. Kim, T.J. Kim

Chonnam National University, Institute for Universe and Elementary Particles, Kwangju, Korea

S. Song

Korea University, Seoul, Korea

S. Cho, S. Choi, Y. Go, D. Gyun, B. Hong, H. Kim, Y. Kim, B. Lee, K. Lee, K.S. Lee, S. Lee, J. Lim, S.K. Park, Y. Roh

Seoul National University, Seoul, Korea

H.D. Yoo

University of Seoul, Seoul, Korea

M. Choi, H. Kim, J.H. Kim, J.S.H. Lee, I.C. Park, G. Ryu, M.S. Ryu

Sungkyunkwan University, Suwon, Korea

Y. Choi, J. Goh, D. Kim, E. Kwon, J. Lee, I. Yu

Vilnius University, Vilnius, Lithuania

V. Dudenas, A. Juodagalvis, J. Vaitkus

National Centre for Particle Physics, Universiti Malaya, Kuala Lumpur, Malaysia

I. Ahmed, Z.A. Ibrahim, J.R. Komaragiri, M.A.B. Md Ali³³, F. Mohamad Idris³⁴, W.A.T. Wan Abdullah, M.N. Yusli, Z. Zolkapli

Centro de Investigacion y de Estudios Avanzados del IPN, Mexico City, Mexico

E. Casimiro Linares, H. Castilla-Valdez, E. De La Cruz-Burelo, I. Heredia-De La Cruz³⁵, A. Hernandez-Almada, R. Lopez-Fernandez, A. Sanchez-Hernandez

Universidad Iberoamericana, Mexico City, Mexico

S. Carrillo Moreno, F. Vazquez Valencia

Benemerita Universidad Autonoma de Puebla, Puebla, Mexico

I. Pedraza, H.A. Salazar Ibarguen, C. Uribe Estrada

Universidad Autónoma de San Luis Potosí, San Luis Potosí, Mexico

A. Morelos Pineda

University of Auckland, Auckland, New Zealand

D. Krofcheck

University of Canterbury, Christchurch, New Zealand

P.H. Butler

National Centre for Physics, Quaid-I-Azam University, Islamabad, Pakistan

A. Ahmad, M. Ahmad, Q. Hassan, H.R. Hoorani, W.A. Khan, T. Khurshid, M. Shoaib, M. Waqas

National Centre for Nuclear Research, Swierk, Poland

H. Bialkowska, M. Bluj, B. Boimska, T. Frueboes, M. Górski, M. Kazana, K. Nawrocki, K. Romanowska-Rybinska, M. Szleper, P. Zalewski

Institute of Experimental Physics, Faculty of Physics, University of Warsaw, Warsaw, Poland

G. Brona, K. Bunkowski, A. Byszuk³⁶, K. Doroba, A. Kalinowski, M. Konecki, J. Krolikowski, M. Misiura, M. Olszewski, M. Walczak

Laboratório de Instrumentação e Física Experimental de Partículas, Lisboa, Portugal

P. Bargassa, C. Beirão Da Cruz E Silva, A. Di Francesco, P. Faccioli, P.G. Ferreira Parracho,

M. Gallinaro, J. Hollar, N. Leonardo, L. Lloret Iglesias, F. Nguyen, J. Rodrigues Antunes, J. Seixas, O. Toldaiev, D. Vadrucchio, J. Varela, P. Vischia

Joint Institute for Nuclear Research, Dubna, Russia

S. Afanasiev, P. Bunin, M. Gavrilenko, I. Golutvin, I. Gorbunov, A. Kamenev, V. Karjavin, A. Lanev, A. Malakhov, V. Matveev^{37,38}, P. Moiseenz, V. Palichik, V. Perelygin, S. Shmatov, S. Shulha, N. Skatchkov, V. Smirnov, A. Zarubin

Petersburg Nuclear Physics Institute, Gatchina (St. Petersburg), Russia

V. Golovtsov, Y. Ivanov, V. Kim³⁹, E. Kuznetsova, P. Levchenko, V. Murzin, V. Oreshkin, I. Smirnov, V. Sulimov, L. Uvarov, S. Vavilov, A. Vorobyev

Institute for Nuclear Research, Moscow, Russia

Yu. Andreev, A. Dermenev, S. Gninenko, N. Golubev, A. Karneyeu, M. Kirsanov, N. Krasnikov, A. Pashenkov, D. Tlisov, A. Toropin

Institute for Theoretical and Experimental Physics, Moscow, Russia

V. Epshteyn, V. Gavrillov, N. Lychkovskaya, V. Popov, I. Pozdnyakov, G. Safronov, A. Spiridonov, E. Vlasov, A. Zhokin

National Research Nuclear University 'Moscow Engineering Physics Institute' (MEPhI), Moscow, Russia

A. Bylinkin, M. Chadeeva, R. Chistov, M. Danilov, V. Rusinov

P.N. Lebedev Physical Institute, Moscow, Russia

V. Andreev, M. Azarkin³⁸, I. Dremin³⁸, M. Kirakosyan, A. Leonidov³⁸, G. Mesyats, S.V. Rusakov

Skobeltsyn Institute of Nuclear Physics, Lomonosov Moscow State University, Moscow, Russia

A. Baskakov, A. Belyaev, E. Boos, V. Bunichev, M. Dubinin⁴⁰, L. Dudko, A. Gribushin, V. Klyukhin, O. Kodolova, N. Korneeva, I. Lokhtin, I. Miagkov, S. Obraztsov, M. Perfilov, V. Savrin

State Research Center of Russian Federation, Institute for High Energy Physics, Protvino, Russia

I. Azhgirey, I. Bayshev, S. Bitioukov, V. Kachanov, A. Kalinin, D. Konstantinov, V. Krychkin, V. Petrov, R. Ryutin, A. Sobol, L. Tourtchanovitch, S. Troshin, N. Tyurin, A. Uzunian, A. Volkov

University of Belgrade, Faculty of Physics and Vinca Institute of Nuclear Sciences, Belgrade, Serbia

P. Adzic⁴¹, P. Cirkovic, D. Devetak, J. Milosevic, V. Rekovic

Centro de Investigaciones Energéticas Medioambientales y Tecnológicas (CIEMAT), Madrid, Spain

J. Alcaraz Maestre, E. Calvo, M. Cerrada, M. Chamizo Llatas, N. Colino, B. De La Cruz, A. Delgado Peris, A. Escalante Del Valle, C. Fernandez Bedoya, J.P. Fernández Ramos, J. Flix, M.C. Fouz, P. Garcia-Abia, O. Gonzalez Lopez, S. Goy Lopez, J.M. Hernandez, M.I. Josa, E. Navarro De Martino, A. Pérez-Calero Yzquierdo, J. Puerta Pelayo, A. Quintario Olmeda, I. Redondo, L. Romero, J. Santaolalla, M.S. Soares

Universidad Autónoma de Madrid, Madrid, Spain

C. Albajar, J.F. de Trocóniz, M. Missiroli, D. Moran

Universidad de Oviedo, Oviedo, Spain

J. Cuevas, J. Fernandez Menendez, S. Folgueras, I. Gonzalez Caballero, E. Palencia Cortezon, J.M. Vizan Garcia

Instituto de Física de Cantabria (IFCA), CSIC-Universidad de Cantabria, Santander, Spain

I.J. Cabrillo, A. Calderon, J.R. Castiñeiras De Saa, P. De Castro Manzano, M. Fernandez, J. Garcia-Ferrero, G. Gomez, A. Lopez Virto, J. Marco, R. Marco, C. Martinez Rivero, F. Matorras, J. Piedra Gomez, T. Rodrigo, A.Y. Rodríguez-Marrero, A. Ruiz-Jimeno, L. Scodellaro, N. Trevisani, I. Vila, R. Vilar Cortabitarte

CERN, European Organization for Nuclear Research, Geneva, Switzerland

D. Abbaneo, E. Auffray, G. Auzinger, M. Bachtis, P. Baillon, A.H. Ball, D. Barney, A. Benaglia, J. Bendavid, L. Benhabib, G.M. Berruti, P. Bloch, A. Bocci, A. Bonato, C. Botta, H. Breuker, T. Camporesi, R. Castello, G. Cerminara, M. D'Alfonso, D. d'Enterria, A. Dabrowski, V. Daponte, A. David, M. De Gruttola, F. De Guio, A. De Roeck, S. De Visscher, E. Di Marco⁴², M. Dobson, M. Dordevic, B. Dorney, T. du Pree, D. Duggan, M. Dünser, N. Dupont, A. Elliott-Peisert, G. Franzoni, J. Fulcher, W. Funk, D. Gigi, K. Gill, D. Giordano, M. Girone, F. Glege, R. Guida, S. Gundacker, M. Guthoff, J. Hammer, P. Harris, J. Hegeman, V. Innocente, P. Janot, H. Kirschenmann, M.J. Kortelainen, K. Kousouris, K. Krajczar, P. Lecoq, C. Lourenço, M.T. Lucchini, N. Magini, L. Malgeri, M. Mannelli, A. Martelli, L. Masetti, F. Meijers, S. Mersi, E. Meschi, F. Moortgat, S. Morovic, M. Mulders, M.V. Nemallapudi, H. Neugebauer, S. Orfanelli⁴³, L. Orsini, L. Pape, E. Perez, M. Peruzzi, A. Petrilli, G. Petrucciani, A. Pfeiffer, M. Pierini, D. Piparo, A. Racz, T. Reis, G. Rolandi⁴⁴, M. Rovere, M. Ruan, H. Sakulin, C. Schäfer, C. Schwick, M. Seidel, A. Sharma, P. Silva, M. Simon, P. Sphicas⁴⁵, J. Steggemann, B. Stieger, M. Stoye, Y. Takahashi, D. Treille, A. Triossi, A. Tsirou, G.I. Veres²¹, N. Wardle, H.K. Wöhri, A. Zagodzinska³⁶, W.D. Zeuner

Paul Scherrer Institut, Villigen, Switzerland

W. Bertl, K. Deiters, W. Erdmann, R. Horisberger, Q. Ingram, H.C. Kaestli, D. Kotlinski, U. Langenegger, T. Rohe

Institute for Particle Physics, ETH Zurich, Zurich, Switzerland

F. Bachmair, L. Bäni, L. Bianchini, B. Casal, G. Dissertori, M. Dittmar, M. Donegà, P. Eller, C. Grab, C. Heidegger, D. Hits, J. Hoss, G. Kasieczka, P. Lecomte[†], W. Lustermann, B. Mangano, M. Marionneau, P. Martinez Ruiz del Arbol, M. Masciovecchio, M.T. Meinhard, D. Meister, F. Micheli, P. Musella, F. Nessi-Tedaldi, F. Pandolfi, J. Pata, F. Pauss, L. Perrozzi, M. Quitnat, M. Rossini, M. Schönenberger, A. Starodumov⁴⁶, M. Takahashi, V.R. Tavolaro, K. Theofilatos, R. Wallny

Universität Zürich, Zurich, Switzerland

T.K. Aarrestad, C. AMSler⁴⁷, L. Caminada, M.F. Canelli, V. Chiochia, A. De Cosa, C. Galloni, A. Hinzmann, T. Hreus, B. Kilminster, C. Lange, J. Ngadiuba, D. Pinna, G. Rauco, P. Robmann, D. Salerno, Y. Yang

National Central University, Chung-Li, Taiwan

M. Cardaci, K.H. Chen, T.H. Doan, Sh. Jain, R. Khurana, M. Konyushikhin, C.M. Kuo, W. Lin, Y.J. Lu, A. Pozdnyakov, S.S. Yu

National Taiwan University (NTU), Taipei, Taiwan

Arun Kumar, P. Chang, Y.H. Chang, Y.W. Chang, Y. Chao, K.F. Chen, P.H. Chen, C. Dietz, F. Fiori, U. Grundler, W.-S. Hou, Y. Hsiung, Y.F. Liu, R.-S. Lu, M. Miñano Moya, E. Petrakou, J.f. Tsai, Y.M. Tzeng

Chulalongkorn University, Faculty of Science, Department of Physics, Bangkok, Thailand

B. Asavapibhop, K. Kovitanggoon, G. Singh, N. Srimanobhas, N. Suwonjandee

Cukurova University, Adana, Turkey

A. Adiguzel, S. Cerci⁴⁸, S. Damarseckin, Z.S. Demiroglu, C. Dozen, I. Dumanoglu, F.H. Gecit, S. Girgis, G. Gokbulut, Y. Guler, E. Gurpinar, I. Hos, E.E. Kangal⁴⁹, A. Kayis Topaksu, G. Onengut⁵⁰, M. Ozcan, K. Ozdemir⁵¹, S. Ozturk⁵², B. Tali⁴⁸, H. Topakli⁵², C. Zorbilmez

Middle East Technical University, Physics Department, Ankara, Turkey

B. Bilin, S. Bilmis, B. Isildak⁵³, G. Karapinar⁵⁴, M. Yalvac, M. Zeyrek

Bogazici University, Istanbul, Turkey

E. Gülmez, M. Kaya⁵⁵, O. Kaya⁵⁶, E.A. Yetkin⁵⁷, T. Yetkin⁵⁸

Istanbul Technical University, Istanbul, Turkey

A. Cakir, K. Cankocak, S. Sen⁵⁹, F.I. Vardarli

Institute for Scintillation Materials of National Academy of Science of Ukraine, Kharkov, Ukraine

B. Grynyov

National Scientific Center, Kharkov Institute of Physics and Technology, Kharkov, Ukraine

L. Levchuk, P. Sorokin

University of Bristol, Bristol, United Kingdom

R. Aggleton, F. Ball, L. Beck, J.J. Brooke, E. Clement, D. Cussans, H. Flacher, J. Goldstein, M. Grimes, G.P. Heath, H.F. Heath, J. Jacob, L. Kreczko, C. Lucas, Z. Meng, D.M. Newbold⁶⁰, S. Paramesvaran, A. Poll, T. Sakuma, S. Seif El Nasr-storey, S. Senkin, D. Smith, V.J. Smith

Rutherford Appleton Laboratory, Didcot, United Kingdom

K.W. Bell, A. Belyaev⁶¹, C. Brew, R.M. Brown, L. Calligaris, D. Cieri, D.J.A. Cockerill, J.A. Coughlan, K. Harder, S. Harper, E. Olaiya, D. Petyt, C.H. Shepherd-Themistocleous, A. Thea, I.R. Tomalin, T. Williams, S.D. Worm

Imperial College, London, United Kingdom

M. Baber, R. Bainbridge, O. Buchmuller, A. Bundock, D. Burton, S. Casasso, M. Citron, D. Colling, L. Corpe, P. Dauncey, G. Davies, A. De Wit, M. Della Negra, P. Dunne, A. Elwood, D. Futyan, G. Hall, G. Iles, R. Lane, R. Lucas⁶⁰, L. Lyons, A.-M. Magnan, S. Malik, J. Nash, A. Nikitenko⁴⁶, J. Pela, M. Pesaresi, D.M. Raymond, A. Richards, A. Rose, C. Seez, A. Tapper, K. Uchida, M. Vazquez Acosta⁶², T. Virdee, S.C. Zenz

Brunel University, Uxbridge, United Kingdom

J.E. Cole, P.R. Hobson, A. Khan, P. Kyberd, D. Leslie, I.D. Reid, P. Symonds, L. Teodorescu, M. Turner

Baylor University, Waco, USA

A. Borzou, K. Call, J. Dittmann, K. Hatakeyama, H. Liu, N. Pastika

The University of Alabama, Tuscaloosa, USA

O. Charaf, S.I. Cooper, C. Henderson, P. Rumerio

Boston University, Boston, USA

D. Arcaro, A. Avetisyan, T. Bose, D. Gastler, D. Rankin, C. Richardson, J. Rohlf, L. Sulak, D. Zou

Brown University, Providence, USA

J. Alimena, G. Benelli, E. Berry, D. Cutts, A. Ferapontov, A. Garabedian, J. Hakala, U. Heintz, O. Jesus, E. Laird, G. Landsberg, Z. Mao, M. Narain, S. Piperov, S. Sagir, R. Syarif

University of California, Davis, Davis, USA

R. Breedon, G. Breto, M. Calderon De La Barca Sanchez, S. Chauhan, M. Chertok, J. Conway, R. Conway, P.T. Cox, R. Erbacher, G. Funk, M. Gardner, W. Ko, R. Lander, C. Mclean, M. Mulhearn, D. Pellett, J. Pilot, F. Ricci-Tam, S. Shalhout, J. Smith, M. Squires, D. Stolp, M. Tripathi, S. Wilbur, R. Yohay

University of California, Los Angeles, USA

R. Cousins, P. Everaerts, A. Florent, J. Hauser, M. Ignatenko, D. Saltzberg, E. Takasugi, V. Valuev, M. Weber

University of California, Riverside, Riverside, USA

K. Burt, R. Clare, J. Ellison, J.W. Gary, G. Hanson, J. Heilman, M. Ivova PANEVA, P. Jandir, E. Kennedy, F. Lacroix, O.R. Long, M. Malberti, M. Olmedo Negrete, A. Shrinivas, H. Wei, S. Wimpenny, B. R. Yates

University of California, San Diego, La Jolla, USA

J.G. Branson, G.B. Cerati, S. Cittolin, R.T. D'Agnolo, M. Derdzinski, A. Holzner, R. Kelley, D. Klein, J. Letts, I. Macneill, D. Olivito, S. Padhi, M. Pieri, M. Sani, V. Sharma, S. Simon, M. Tadel, A. Vartak, S. Wasserbaech⁶³, C. Welke, F. Würthwein, A. Yagil, G. Zevi Della Porta

University of California, Santa Barbara, Santa Barbara, USA

J. Bradmiller-Feld, C. Campagnari, A. Dishaw, V. Dutta, K. Flowers, M. Franco Sevilla, P. Geffert, C. George, F. Golf, L. Gouskos, J. Gran, J. Incandela, N. Mccoll, S.D. Mullin, J. Richman, D. Stuart, I. Suarez, C. West, J. Yoo

California Institute of Technology, Pasadena, USA

D. Anderson, A. Apresyan, A. Bornheim, J. Bunn, Y. Chen, J. Duarte, A. Mott, H.B. Newman, C. Pena, M. Spiropulu, J.R. Vlimant, S. Xie, R.Y. Zhu

Carnegie Mellon University, Pittsburgh, USA

M.B. Andrews, V. Azzolini, A. Calamba, B. Carlson, T. Ferguson, M. Paulini, J. Russ, M. Sun, H. Vogel, I. Vorobiev

University of Colorado Boulder, Boulder, USA

J.P. Cumalat, W.T. Ford, A. Gaz, F. Jensen, A. Johnson, M. Krohn, T. Mulholland, U. Nauenberg, K. Stenson, S.R. Wagner

Cornell University, Ithaca, USA

J. Alexander, A. Chatterjee, J. Chaves, J. Chu, S. Dittmer, N. Eggert, N. Mirman, G. Nicolas Kaufman, J.R. Patterson, A. Rinkevicius, A. Ryd, L. Skinnari, L. Soffi, W. Sun, S.M. Tan, W.D. Teo, J. Thom, J. Thompson, J. Tucker, Y. Weng, P. Wittich

Fermi National Accelerator Laboratory, Batavia, USA

S. Abdullin, M. Albrow, G. Apollinari, S. Banerjee, L.A.T. Bauerdick, A. Beretvas, J. Berryhill, P.C. Bhat, G. Bolla, K. Burkett, J.N. Butler, H.W.K. Cheung, F. Chlebana, S. Cihangir, V.D. Elvira, I. Fisk, J. Freeman, E. Gottschalk, L. Gray, D. Green, S. Grünendahl, O. Gutsche, J. Hanlon, D. Hare, R.M. Harris, S. Hasegawa, J. Hirschauer, Z. Hu, B. Jayatilaka, S. Jindariani, M. Johnson, U. Joshi, B. Klima, B. Kreis, S. Lammel, J. Lewis, J. Linacre, D. Lincoln, R. Lipton, T. Liu, R. Lopes De Sá, J. Lykken, K. Maeshima, J.M. Marraffino, S. Maruyama, D. Mason, P. McBride, P. Merkel, S. Mrenna, S. Nahn, C. Newman-Holmes[†], V. O'Dell, K. Pedro, O. Prokofyev,

G. Rakness, E. Sexton-Kennedy, A. Soha, W.J. Spalding, L. Spiegel, S. Stoynev, N. Strobbe, L. Taylor, S. Tkaczyk, N.V. Tran, L. Uplegger, E.W. Vaandering, C. Vernieri, M. Verzocchi, R. Vidal, M. Wang, H.A. Weber, A. Whitbeck

University of Florida, Gainesville, USA

D. Acosta, P. Avery, P. Bortignon, D. Bourilkov, A. Brinkerhoff, A. Carnes, M. Carver, D. Curry, S. Das, R.D. Field, I.K. Furic, S.V. Gleyzer, J. Konigsberg, A. Korytov, K. Kotov, P. Ma, K. Matchev, H. Mei, P. Milenovic⁶⁴, G. Mitselmakher, D. Rank, R. Rossin, L. Shchutska, M. Snowball, D. Sperka, N. Terentyev, L. Thomas, J. Wang, S. Wang, J. Yelton

Florida International University, Miami, USA

S. Hewamanage, S. Linn, P. Markowitz, G. Martinez, J.L. Rodriguez

Florida State University, Tallahassee, USA

A. Ackert, J.R. Adams, T. Adams, A. Askew, S. Bein, J. Bochenek, B. Diamond, J. Haas, S. Hagopian, V. Hagopian, K.F. Johnson, A. Khatiwada, H. Prosper, M. Weinberg

Florida Institute of Technology, Melbourne, USA

M.M. Baarmand, V. Bhopatkar, S. Colafranceschi⁶⁵, M. Hohlmann, H. Kalakhety, D. Noonan, T. Roy, F. Yumiceva

University of Illinois at Chicago (UIC), Chicago, USA

M.R. Adams, L. Apanasevich, D. Berry, R.R. Betts, I. Bucinskaite, R. Cavanaugh, O. Evdokimov, L. Gauthier, C.E. Gerber, D.J. Hofman, P. Kurt, C. O'Brien, I.D. Sandoval Gonzalez, P. Turner, N. Varelas, Z. Wu, M. Zakaria, J. Zhang

The University of Iowa, Iowa City, USA

B. Bilki⁶⁶, W. Clarida, K. Dilsiz, S. Durgut, R.P. Gandrajula, M. Haytmyradov, V. Khristenko, J.-P. Merlo, H. Mermerkaya⁶⁷, A. Mestvirishvili, A. Moeller, J. Nachtman, H. Ogul, Y. Onel, F. Ozok⁶⁸, A. Penzo, C. Snyder, E. Tiras, J. Wetzel, K. Yi

Johns Hopkins University, Baltimore, USA

I. Anderson, B.A. Barnett, B. Blumenfeld, N. Eminizer, D. Fehling, L. Feng, A.V. Gritsan, P. Maksimovic, M. Osherson, J. Roskes, A. Sady, U. Sarica, M. Swartz, M. Xiao, Y. Xin, C. You

The University of Kansas, Lawrence, USA

P. Baringer, A. Bean, C. Bruner, R.P. Kenny III, D. Majumder, M. Malek, W. Mcbrayer, M. Murray, S. Sanders, R. Stringer, Q. Wang

Kansas State University, Manhattan, USA

A. Ivanov, K. Kaadze, S. Khalil, M. Makouski, Y. Maravin, A. Mohammadi, L.K. Saini, N. Skhirtladze, S. Toda

Lawrence Livermore National Laboratory, Livermore, USA

D. Lange, F. Rebassoo, D. Wright

University of Maryland, College Park, USA

C. Anelli, A. Baden, O. Baron, A. Belloni, B. Calvert, S.C. Eno, C. Ferraioli, J.A. Gomez, N.J. Hadley, S. Jabeen, G.Y. Jeng⁶⁹, R.G. Kellogg, T. Kolberg, J. Kunkle, Y. Lu, A.C. Mignerey, Y.H. Shin, A. Skuja, M.B. Tonjes, S.C. Tonwar

Massachusetts Institute of Technology, Cambridge, USA

A. Apyan, R. Barbieri, A. Baty, R. Bi, K. Bierwagen, S. Brandt, W. Busza, I.A. Cali, Z. Demiragli, L. Di Matteo, G. Gomez Ceballos, M. Goncharov, D. Gulhan, Y. Iiyama, G.M. Innocenti, M. Klute, D. Kovalskyi, Y.S. Lai, Y.-J. Lee, A. Levin, P.D. Luckey, A.C. Marini, C. Mcginn,

C. Mironov, S. Narayanan, X. Niu, C. Paus, C. Roland, G. Roland, J. Salfeld-Nebgen, G.S.F. Stephans, K. Sumorok, M. Varma, D. Velicanu, J. Veverka, J. Wang, T.W. Wang, B. Wyslouch, M. Yang, V. Zhukova

University of Minnesota, Minneapolis, USA

A.C. Benvenuti, B. Dahmes, A. Evans, A. Finkel, A. Gude, P. Hansen, S. Kalafut, S.C. Kao, K. Klapoetke, Y. Kubota, Z. Lesko, J. Mans, S. Nourbakhsh, N. Ruckstuhl, R. Rusack, N. Tambe, J. Turkewitz

University of Mississippi, Oxford, USA

J.G. Acosta, S. Oliveros

University of Nebraska-Lincoln, Lincoln, USA

E. Avdeeva, R. Bartek, K. Bloom, S. Bose, D.R. Claes, A. Dominguez, C. Fangmeier, R. Gonzalez Suarez, R. Kamalieddin, D. Knowlton, I. Kravchenko, F. Meier, J. Monroy, F. Ratnikov, J.E. Siado, G.R. Snow

State University of New York at Buffalo, Buffalo, USA

M. Alyari, J. Dolen, J. George, A. Godshalk, C. Harrington, I. Iashvili, J. Kaisen, A. Kharchilava, A. Kumar, S. Rappoccio, B. Roozbahani

Northeastern University, Boston, USA

G. Alverson, E. Barberis, D. Baumgartel, M. Chasco, A. Hortiangtham, A. Massironi, D.M. Morse, D. Nash, T. Orimoto, R. Teixeira De Lima, D. Trocino, R.-J. Wang, D. Wood, J. Zhang

Northwestern University, Evanston, USA

S. Bhattacharya, K.A. Hahn, A. Kubik, J.F. Low, N. Mucia, N. Odell, B. Pollack, M. Schmitt, K. Sung, M. Trovato, M. Velasco

University of Notre Dame, Notre Dame, USA

N. Dev, M. Hildreth, C. Jessop, D.J. Karmgard, N. Kellams, K. Lannon, N. Marinelli, F. Meng, C. Mueller, Y. Musienko³⁷, M. Planer, A. Reinsvold, R. Ruchti, G. Smith, S. Taroni, N. Valls, M. Wayne, M. Wolf, A. Woodard

The Ohio State University, Columbus, USA

L. Antonelli, J. Brinson, B. Bylsma, L.S. Durkin, S. Flowers, A. Hart, C. Hill, R. Hughes, W. Ji, T.Y. Ling, B. Liu, W. Luo, D. Puigh, M. Rodenburg, B.L. Winer, H.W. Wulsin

Princeton University, Princeton, USA

O. Driga, P. Elmer, J. Hardenbrook, P. Hebda, S.A. Koay, P. Lujan, D. Marlow, T. Medvedeva, M. Mooney, J. Olsen, C. Palmer, P. Piroué, D. Stickland, C. Tully, A. Zuranski

University of Puerto Rico, Mayaguez, USA

S. Malik

Purdue University, West Lafayette, USA

A. Barker, V.E. Barnes, D. Benedetti, D. Bortoletto, L. Gutay, M.K. Jha, M. Jones, A.W. Jung, K. Jung, A. Kumar, D.H. Miller, N. Neumeister, B.C. Radburn-Smith, X. Shi, I. Shipsey, D. Silvers, J. Sun, A. Svyatkovskiy, F. Wang, W. Xie, L. Xu

Purdue University Calumet, Hammond, USA

N. Parashar, J. Stupak

Rice University, Houston, USA

A. Adair, B. Akgun, Z. Chen, K.M. Ecklund, F.J.M. Geurts, M. Guilbaud, W. Li, B. Michlin, M. Northup, B.P. Padley, R. Redjimi, J. Roberts, J. Rorie, Z. Tu, J. Zabel

University of Rochester, Rochester, USA

B. Betchart, A. Bodek, P. de Barbaro, R. Demina, Y. Eshaq, T. Ferbel, M. Galanti, A. Garcia-Bellido, J. Han, A. Harel, O. Hindrichs, A. Khukhunaishvili, K.H. Lo, G. Petrillo, P. Tan, M. Verzetti

Rutgers, The State University of New Jersey, Piscataway, USA

J.P. Chou, E. Contreras-Campana, D. Ferencek, Y. Gershtein, E. Halkiadakis, M. Heindl, D. Hidas, E. Hughes, S. Kaplan, R. Kunnawalkam Elayavalli, A. Lath, K. Nash, H. Saka, S. Salur, S. Schnetzer, D. Sheffield, S. Somalwar, R. Stone, S. Thomas, P. Thomassen, M. Walker

University of Tennessee, Knoxville, USA

M. Foerster, G. Riley, K. Rose, S. Spanier, K. Thapa

Texas A&M University, College Station, USA

O. Bouhali⁷⁰, A. Castaneda Hernandez⁷⁰, A. Celik, M. Dalchenko, M. De Mattia, A. Delgado, S. Dildick, R. Eusebi, J. Gilmore, T. Huang, T. Kamon⁷¹, V. Krutelyov, R. Mueller, I. Osipenkov, Y. Pakhotin, R. Patel, A. Perloff, A. Rose, A. Safonov, A. Tatarinov, K.A. Ulmer²

Texas Tech University, Lubbock, USA

N. Akchurin, C. Cowden, J. Damgov, C. Dragoiu, P.R. Duerdo, J. Faulkner, S. Kunori, K. Lamichhane, S.W. Lee, T. Libeiro, S. Undleeb, I. Volobouev

Vanderbilt University, Nashville, USA

E. Appelt, A.G. Delannoy, S. Greene, A. Gurrola, R. Janjam, W. Johns, C. Maguire, Y. Mao, A. Melo, H. Ni, P. Sheldon, S. Tuo, J. Velkovska, Q. Xu

University of Virginia, Charlottesville, USA

M.W. Arenton, B. Cox, B. Francis, J. Goodell, R. Hirosky, A. Ledovskoy, H. Li, C. Lin, C. Neu, T. Sinthuprasith, X. Sun, Y. Wang, E. Wolfe, J. Wood, F. Xia

Wayne State University, Detroit, USA

C. Clarke, R. Harr, P.E. Karchin, C. Kottachchi Kankanamge Don, P. Lamichhane, J. Sturdy

University of Wisconsin - Madison, Madison, WI, USA

D.A. Belknap, D. Carlsmith, M. Cepeda, S. Dasu, L. Dodd, S. Duric, B. Gomber, M. Grothe, M. Herndon, A. Hervé, P. Klabbers, A. Lanaro, A. Levine, K. Long, R. Loveless, A. Mohapatra, I. Ojalvo, T. Perry, G.A. Pierro, G. Polese, T. Ruggles, T. Sarangi, A. Savin, A. Sharma, N. Smith, W.H. Smith, D. Taylor, P. Verwilligen, N. Woods

†: Deceased

1: Also at Vienna University of Technology, Vienna, Austria

2: Also at CERN, European Organization for Nuclear Research, Geneva, Switzerland

3: Also at State Key Laboratory of Nuclear Physics and Technology, Peking University, Beijing, China

4: Also at Institut Pluridisciplinaire Hubert Curien, Université de Strasbourg, Université de Haute Alsace Mulhouse, CNRS/IN2P3, Strasbourg, France

5: Also at National Institute of Chemical Physics and Biophysics, Tallinn, Estonia

6: Also at Skobeltsyn Institute of Nuclear Physics, Lomonosov Moscow State University, Moscow, Russia

7: Also at Universidade Estadual de Campinas, Campinas, Brazil

- 8: Also at Centre National de la Recherche Scientifique (CNRS) - IN2P3, Paris, France
- 9: Also at Laboratoire Leprince-Ringuet, Ecole Polytechnique, IN2P3-CNRS, Palaiseau, France
- 10: Also at Joint Institute for Nuclear Research, Dubna, Russia
- 11: Also at Helwan University, Cairo, Egypt
- 12: Now at Zewail City of Science and Technology, Zewail, Egypt
- 13: Also at British University in Egypt, Cairo, Egypt
- 14: Now at Ain Shams University, Cairo, Egypt
- 15: Also at Université de Haute Alsace, Mulhouse, France
- 16: Also at Tbilisi State University, Tbilisi, Georgia
- 17: Also at RWTH Aachen University, III. Physikalisches Institut A, Aachen, Germany
- 18: Also at University of Hamburg, Hamburg, Germany
- 19: Also at Brandenburg University of Technology, Cottbus, Germany
- 20: Also at Institute of Nuclear Research ATOMKI, Debrecen, Hungary
- 21: Also at Eötvös Loránd University, Budapest, Hungary
- 22: Also at University of Debrecen, Debrecen, Hungary
- 23: Also at Wigner Research Centre for Physics, Budapest, Hungary
- 24: Also at Indian Institute of Science Education and Research, Bhopal, India
- 25: Also at University of Visva-Bharati, Santiniketan, India
- 26: Now at King Abdulaziz University, Jeddah, Saudi Arabia
- 27: Also at University of Ruhuna, Matara, Sri Lanka
- 28: Also at Isfahan University of Technology, Isfahan, Iran
- 29: Also at University of Tehran, Department of Engineering Science, Tehran, Iran
- 30: Also at Plasma Physics Research Center, Science and Research Branch, Islamic Azad University, Tehran, Iran
- 31: Also at Università degli Studi di Siena, Siena, Italy
- 32: Also at Purdue University, West Lafayette, USA
- 33: Also at International Islamic University of Malaysia, Kuala Lumpur, Malaysia
- 34: Also at Malaysian Nuclear Agency, MOSTI, Kajang, Malaysia
- 35: Also at Consejo Nacional de Ciencia y Tecnología, Mexico city, Mexico
- 36: Also at Warsaw University of Technology, Institute of Electronic Systems, Warsaw, Poland
- 37: Also at Institute for Nuclear Research, Moscow, Russia
- 38: Now at National Research Nuclear University 'Moscow Engineering Physics Institute' (MEPhI), Moscow, Russia
- 39: Also at St. Petersburg State Polytechnical University, St. Petersburg, Russia
- 40: Also at California Institute of Technology, Pasadena, USA
- 41: Also at Faculty of Physics, University of Belgrade, Belgrade, Serbia
- 42: Also at INFN Sezione di Roma; Università di Roma, Roma, Italy
- 43: Also at National Technical University of Athens, Athens, Greece
- 44: Also at Scuola Normale e Sezione dell'INFN, Pisa, Italy
- 45: Also at National and Kapodistrian University of Athens, Athens, Greece
- 46: Also at Institute for Theoretical and Experimental Physics, Moscow, Russia
- 47: Also at Albert Einstein Center for Fundamental Physics, Bern, Switzerland
- 48: Also at Adiyaman University, Adiyaman, Turkey
- 49: Also at Mersin University, Mersin, Turkey
- 50: Also at Cag University, Mersin, Turkey
- 51: Also at Piri Reis University, Istanbul, Turkey
- 52: Also at Gaziosmanpasa University, Tokat, Turkey
- 53: Also at Ozyegin University, Istanbul, Turkey
- 54: Also at Izmir Institute of Technology, Izmir, Turkey

-
- 55: Also at Marmara University, Istanbul, Turkey
56: Also at Kafkas University, Kars, Turkey
57: Also at Istanbul Bilgi University, Istanbul, Turkey
58: Also at Yildiz Technical University, Istanbul, Turkey
59: Also at Hacettepe University, Ankara, Turkey
60: Also at Rutherford Appleton Laboratory, Didcot, United Kingdom
61: Also at School of Physics and Astronomy, University of Southampton, Southampton, United Kingdom
62: Also at Instituto de Astrofísica de Canarias, La Laguna, Spain
63: Also at Utah Valley University, Orem, USA
64: Also at University of Belgrade, Faculty of Physics and Vinca Institute of Nuclear Sciences, Belgrade, Serbia
65: Also at Facoltà Ingegneria, Università di Roma, Roma, Italy
66: Also at Argonne National Laboratory, Argonne, USA
67: Also at Erzincan University, Erzincan, Turkey
68: Also at Mimar Sinan University, Istanbul, Istanbul, Turkey
69: Also at University of Sydney, Sydney, Australia
70: Also at Texas A&M University at Qatar, Doha, Qatar
71: Also at Kyungpook National University, Daegu, Korea